SME Annual Meeting
Feb. 27 - Mar. 02, 2022, Salt Lake City, UT

Preprint 22-033

STRESS MEASUREMENT AND MONITORING IN ANISOTROPIC ROCK

W. G. Pariseau, Univ. of Utah, Salt Lake City, UT

INTRODUCTION

Reliable stress measurement using hollow inclusion gauges and monitoring stress change using borehole stress meters and borehole deformation gauges in anisotropic rock remains a challenge for the rock mechanics community. In this regard, the complex variable method advanced in 1983 for deducing stress in anisotropic rock is flawed and software is privileged. Fortunately, advances in computer hardware and software now enable fast, reliable reduction of hollow inclusion *stress measurement* data for determining stress in anisotropic rock. Monitoring *stress change* in anisotropic rock poses a different challenge but is also subject to numerical analysis.

Stress measurement using a hollow inclusion (HI) gauge such as the triaxial Australian HI is done in four steps: 1) drilling a measurement hole, 2) installation of an HI, 3) stress relief of the HI by overcoring, and 4) data reduction. The last step, data reduction, is the focus of this work. The process is well-known in linearly elastic, *isotropic* rock (Worotniki and Walton 1976, Duncan Fama and Pender 1980). However, in case of linearly elastic, *anisotropic* rock the requisite technology is not readily available. This situation is somewhat surprising because anisotropy is more often the rule rather than the exception, especially in the neighborhood of ore bodies. Rahn (1984) has pointed out the potential for significant errors with neglect of anisotropy and the adverse consequences for engineering design. Amadei (1984) has also pointed out the potential for errors with neglect of anisotropic rock properties in stress measurement. Worotniki (1993) cites other studies that indicate potential for serious errors when doing measurements in anisotropic rock. In both theoretical cases (isotropy and anisotropy), data reduction is essentially a composite of solutions to boundary value problems in linear elasticity. In the finite element approach, the analysis is a simulation of gauge hole drilling, installation and overcoring. Two important advantages with the finite element approach are a more faithful representation of the conditions of HI stress measurement than approximated in theory and the capability for handling rock whether isotropic, transversely isotropic or fully anisotropic.

A major difficulty in obtaining an analytical solution is imposition of continuity conditions at the interface between gauge and rock. In case of *isotropic* rock a theoretical solution is used for a soft (epoxy) hollow inclusion (Duncan Fama and Pender 1980) that is based on the work by Savin (1961) where a circular hole in a plate (plane stress) is reinforced by concentric rings of different material. These same continuity requirements also complicate the solution in case of anisotropy. While the procedural template is much the same, evidently the anisotropic solution has not been obtained, although a problem somewhat similar to that of Savin (1961) provides a starting point in case of anisotropy (Engles et al 2001). A notable effort by Amadei (1983) dealing with stress measurements in anisotropic rock provides guidance towards an approximate solution after building on the fundamental work of Lekhnitskii (1963). Unfortunately, computer programs in the work by Amadei are not available to the technical community at large and there is reason to suspect the presence of flaws in these rather involved computer programs (Pariseau 1987). There is also an alternative to the formalism of Lekhnitskii and that is a Stroh formalism described at length by Ting (1996), although application to stress measurement is not addressed. In this regard, a general discussion of stress measurement in rock with many useful references at the end of each chapter is given by Amadei and Stephansson (1997).

Two important issues associated with stress monitoring and measurements are: (1) how to determine the three-dimensional state of stress from plane analyses in several holes, and (2) how to determine the elastic moduli, especially in case of anisotropy. The first is addressed in the early literature about stress measurements, e.g., in Obert and Duvall (1967). The second can be addressed by laboratory testing of drill core samples from the formation where measurements are made, e.g., as done in work described in Pariseau et al (1995, 1996). In this work, three mutually orthogonal drill holes were cored down dip, along strike and in a direction normal to foliation to obtain samples that were tested in the laboratory for elastic and strength properties in support of an orthotropic material model. Subsequent field studies demonstrated the practicality of this approach in obtaining high correlations between finite element mine modeling and mine measurements. To be sure, there are numerous descriptions for determining elastic moduli in the transversely isotropic case by testing an overcored hollow cylinder in the usual biaxial chamber or by testing a strain cell ("doorstopper"). However, there are many caveats in such procedures and the frequent assumption of transverse isotropy may not be adequate to a measurement at hand, say, in orthotropic rock. Conceivably and even more complex anisotropy than orthotropy could be required. Given the requisite elastic input data, the degree of anisotropy is not an issue here provided the finite element program of choice uses a six by six material properties matrix[*C*] in the stress – strain relations:

$$\{\sigma\}_{6x1} = [C]_{6x6}\{\varepsilon\}_{6x1}$$

An additional issue is heterogeneity, that is, spatial variability in rock properties. Of course spatial variability exists at several scales in rock mechanics, from a sub-millimeter scale of dislocations and crystal lattice defects, to a millimeter grain scale, to a centimeter gauge scale, to a meter site scale and on to the scale of joint spacing. An associated concern is variability in measurement data, not only along a hole, but between holes as well. Scaling heterogeneity can be addressed in a finite element application using a Monte Carlo approach or perhaps using a stochastic finite element approach. Indeed, a series of publications by a group led by Corthesy et al (2016) describe using the finite element approach for interpretation of "doorstopper" data (Yameogo et al 2013a, 2013 b). In this regard, Corthesy et al (2016) describe recording of strains from a doorstopper gauge during overcoring and thus obtaining the history of strain relief. Inversion of the strains at any point along a gauge overcoring history is possible and indeed 19 such points are used in analyses by a finite element method. A logical hazard in dealing with heterogeneity and variability is to infer absence of anisotropy in laboratory test data because of statistical variability, especially in strength data that often exhibit coefficients of variability greater than 35 percent. A Student's t-test of strength data obtained from core parallel and perpendicular to bedding may not show a statistical difference in means, despite the visible presence of foliation. Elastic moduli data typically show less variation than strength data. A modulus ratio of means of 1.25 may be present but deemed statistically insignificant. So the logical hazard is still present and evident anisotropy certainly should *not* be neglected.

Others have also used the finite element method for stress measurements for another type of hollow inclusion stress gauge (Figueiredo et al 2009). In this regard, reviews and conferences devoted to stress measurement in rock indicate a trend towards greater detail and the proliferation of proprietary computer programs to

handle anisotropy and various types of gauges. Hakala and Sjorberg (2006) have developed a program for stress measurement in anisotropic rock following Lekhnitskii (1963) and Amadei (1983) with application to two types of stress gauges ("*Borre* and *CSIRO HI*"). Focus is on transversely isotropic rock. The program is available through a licensing procedure. Lu (2006) describes a method for interpreting data from a "doorstopper" (also in transversely isotropic rock) a method based on a program DISCO developed at SINTEF and also used in a number of measurement campaigns.

FINITE ELEMENT PROCEDURE - MEASUREMENT

A simple approach to data reduction in anisotropic rock and to solutions of requisite boundary value problems is through application of the well-known finite element method. The most common finite element procedure (Zienkiewicz and Cheung 1967, Desai and Abel 1972, Cook 1974) considers displacements as unknowns in a "stiffness" system of equations: $\{F\}=[K]\{U\}$ where $\{F\},[K]$ and $\{U\}$ are force vector, global stiffness matrix and displacement vector, respectively. In application to excavation in rock, forces are computed from *in situ* stresses $\{\sigma_o\}$. A forward solution process solves for the unknown displacements $\{U\}$ subject to constraints imposed by stress equations of equilibrium (Fung 1965), small strain displacement relations (Love 1944), generalized Hooke's law (Malvern 1969, Jaunzemis 1967), and boundary conditions. Global displacements {*U*} in turn allow for specification of local displacements $\{\delta\}$ associated with individual elements. In common finite element notation, displacements $\{u\}$ within an element are expressed in terms of element nodal displacements $\{\delta\}$ via interpolation functions $[N]$ such that $\{u\}=[N(x,y,z)]\{\delta\}$. Node displacements then allow for computation of element strains $\{\varepsilon\}=[B]\{\delta\}$. Element stresses are easily computed using Hooke's law in anisotropic form (generalized Hooke's law): $\{\sigma\}=[E]\{\varepsilon\}$ where [*E*] is a 6 x 6 symmetric matrix of elastic constants.

Anisotropy of the most general type requires 21 independent elastic moduli (Lekhnitskii 1963, Ting 1996). However, actual measurements to support such a model in rock mechanics are unknown. Orthotropic models of rock anisotropy based on three planes of material symmetry and thus three axes of anisotropy requiring just nine independent elastic constants are most likely sufficient. Some measurements have been made to support an orthotropic model including strength as well as elastic properties (Pariseau *et al* 1995, 1996), although transversely isotropic models are perhaps the most used anisotropic models in rock mechanics and require only five independent elastic constants. Regardless of the model, determination of the elastic constants is necessary to successful data reduction. These constants can be determined using laboratory test procedures on drill core taken from the gauge hole in the vicinity of the gauge site. However, details are beyond the scope of this paper as are operational concerns such as proper preparation of the cement used to bond an HI to a borehole wall. Of course, the conventional pressure testing of the hollow cylinder overcore with the gauge still installed can supplement the laboratory testing for the elastic constants and reveal whether the cement has bonded securely to the HI.

With reference to Figure 1 that shows a cross-section (A) through the center of an HI and a long section (B), overcoring along the dotted line relieves the stress in the overcore and simultaneously strains the HI. The mesh cross-section in Figure 1 is a square 322.1 mm on edge. Hole diameter is 38 mm. Strain gauges are at a radius of 17.5 mm in a HI with an inside radius of 16 mm or 14 mm depending on the HI used. Length of the HI in the mesh is 137 mm. The overcore diameter is 146 mm.

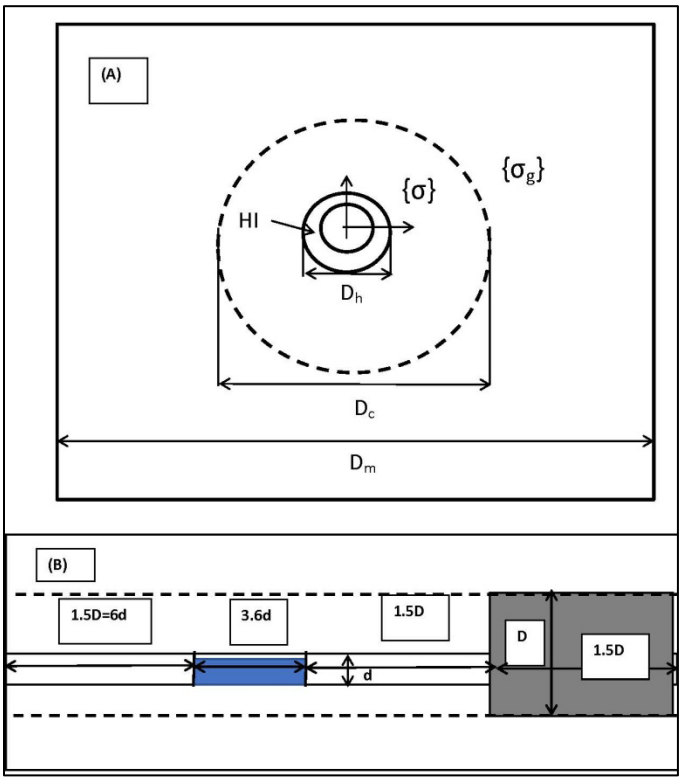

Figure 1. (A) Cross-section schematic of a hollow inclusion (HI) installed in a borehole. (B) long section. Dotted lines indicate overcore. Initial prehole stress is {σ_o}. The inclusion is initially unstressed, but is strained during overcoring that relieves the stress {σ} in the surrounding rock. The overcore length is several times HI length and expands axially as well as laterally during overcoring.

Strains $\{\varepsilon_g\}$ are linearly related to the gauge stress $\{\sigma_g\}$ relieved by overcoring. Thus,

$$\{\varepsilon_g\}=[C]\{\sigma_g\} \text{ and } \{\sigma_g\}=[S]\{\varepsilon_g\} \qquad (1ab)$$

where $\{\varepsilon_g\},[C]$ and $\{\sigma_g\}$ are an *n*x1 column matrix of *n* gauge strains, an *n*x6 HI compliance matrix and a 6x1 column matrix of stresses; $[S]$ is a 6x*n* HI stiffness matrix. The HI matrices $[C]$ and $[S]$ are obtained from finite element analysis. Dimensions of the matrices $[C]$ and $[S]$ depend on the number of strain gauges *n* in the considered HI, but are generally not square and therefore are not mutual inverses. However, "squaring" the system $\{\varepsilon_g\}=[C]\{\sigma_g\}$ allows for "inversion" to obtain $\{\sigma_g\}=[S]\{\varepsilon_g\}$ where

$$[S]=([C]^T[C])^{-1}[C]^T \qquad (2)$$

and the superscript T means transpose. For example, in case of a nine strain gauges in an HI, the dimensions of [*C*] are 9 rows by 6 columns; dimensions of [*S*] are then 6 rows by 9 columns. Although the product matrix $[C]^T[C]$ is symmetric (6x6) and suggests inevitability, there is no guarantee without diagonal dominance. Actual data reduction of an HI is somewhat more involved because of redundant strain measurements that allow for statistical considerations and "best fits". In any case, the small strain attribute of superposition in linear elasticity is the key to the proposed data reduction method.

Construction of $[C]$ begins with application of a unit load in the *x*-direction, say $\sigma_1 = 1000$, to a borehole containing an HI. The result is strain $\{\varepsilon_n^1\}$. The loading process continues until the last of six unit loads have been computed in turn. The final result is the $[C]$ matrix. Thus,

$$[C] = \begin{bmatrix} \varepsilon_1^1/\sigma_1 & \varepsilon_1^2/\sigma_2 & \ldots & \varepsilon_1^6/\sigma_6 \\ \varepsilon_2^1/\sigma_1 & \varepsilon_2^2/\sigma_2 & \ldots & \varepsilon_2^6/\sigma_6 \\ & & \ldots & \\ \varepsilon_n^1/\sigma_1 & \varepsilon_n^2/\sigma_2 & \ldots & \varepsilon_n^6/\sigma_6 \end{bmatrix} \quad (3a)$$

that is,

$$C_{ij} = \varepsilon_i / \sigma_j \qquad (i = 1, n \text{ and } j = 1, 6) \quad (3b)$$

Superposition of the effects of the six unit stress loads on strains is obtained by *n*-row sums. Thus,

$$\{\varepsilon_g\} = \sum_{j=1,6} \varepsilon_{ij} \quad (4)$$

A simple check on the procedure is the computation $\{\sigma_h\} = [S]\{\varepsilon_g\}$ where the subscript *h* implies premining stress relative to hole coordinates. If unit stresses were applied, then the check should show $\{\sigma_h\} = \{111111\}$. If some other loading were applied, say, {6 5 4 3 2 1}, then $\{\sigma_h\} = [S]\{\varepsilon_g\} = \{654321\}$ using the *original* $[S]$ matrix, the one computed using unit loads. The reason is found in linearity of the elastic material model.

Transformation of hole stress $\{\sigma_h\}$ to *in situ* stress $\{\sigma_o\}$ relative to a global, say, mine coordinates or compass coordinates *xyz* (x=East, y=North, z=Up) is readily done with the transformation matrix [T_{oh}] such that $\{\sigma_o\} = [T_{oh}]\{\sigma_h\}$, that is, $\{\sigma_o\} = [S_o]\{\varepsilon_g\}$ where $[S_o] = [T_{oh}][S]$.

Data reduction proceeds in three simple steps: (1) preparation of an input data file, (2) execution of the finite element program and (3) computation of the *in situ* stress state. An example illustrates the procedure; reliability of the program is demonstrated in Appendix A. Influence of cement is briefly discussed in Appendix B.

Step 1 Input File

The input data file contains the elastic moduli of rock informed by a generalized Hooke's law. Azimuth and inclination of the axes of anisotropy with respect to the finite element axes are required input; azimuth and inclination of the drill hole containing the HI are also required. The number of strain gauges in the considered HI is usually 9, but may be 12 in practice. Elastic moduli of the HI and in this study the elastic moduli of the cement used to bond the HI to the rock are also required. These data allow for flexible and stiff HI's, cement, and rock in various combinations.

Generalized Hooke's law is $\{\varepsilon\} = [E]\{\sigma\}$ where $\{\varepsilon\}$, $[E]$ and $\{\sigma\}$ are a 6x1 column matrix of strain, a fully populated 6x6 symmetric matrix of elastic constants, and a 6x1 column matrix of stress, respectively. In case of material with three mutually orthogonal axes of symmetry (orthotropic, 9–constant model), generalized Hooke's law for linearly elastic geologic media is referred to the axes of anisotropy *abc* is in matrix form

$$\begin{Bmatrix} \varepsilon_{aa} \\ \varepsilon_{bb} \\ \varepsilon_{cc} \\ \gamma_{bc} \\ \gamma_{ca} \\ \gamma_{ab} \end{Bmatrix} = \begin{bmatrix} 1/E_{aa} & -\nu_{ba}/E_{bb} & -\nu_{ca}/E_{cc} & 0 & 0 & 0 \\ -\nu_{ab}/E_{aa} & 1/E_{bb} & -\nu_{cb}/E_{cc} & 0 & 0 & 0 \\ -\nu_{ac}/E_{aa} & -\nu_{bc}/E_{bb} & 1/E_{cc} & 0 & 0 & 0 \\ 0 & 0 & 0 & 1/G_{ab} & 0 & 0 \\ 0 & 0 & 0 & 0 & 1/G_{bc} & 0 \\ 0 & 0 & 0 & 0 & 0 & 1/G_{ca} \end{bmatrix} \begin{Bmatrix} \sigma_{aa} \\ \sigma_{bb} \\ \sigma_{cc} \\ \tau_{bc} \\ \tau_{ca} \\ \tau_{ab} \end{Bmatrix} \quad (5)$$

Symmetry requires $\nu_{ba}/E_{bb} = \nu_{ab}/E_{aa}$ and so forth. The corresponding finite element input properties data file layout is given in Table 1.

Table 1. Layout of rock properties files.

Rock Type					
E_{aa}	E_{bb}	E_{cc}	ν_{ab}	ν_{bc}	ν_{ca}
G_{ab}	G_{bc}	G_{ca}			
α-abc	δ-abc	α-hole	δ-hole		
HI					
E_{aa}	E_{bb}	E_{cc}	ν_{ab}	ν_{bc}	ν_{ca}
G_{ab}	G_{bc}	G_{ca}			

Where E's, v's and G's are Young's moduli, Poisson's ratios and shear moduli, respectively; α-abc and δ-abc are azimuth and dip (+ down) of the a-axis of anisotropy; α-hole and δ-hole are an azimuth and inclination (+ up) of the HI hole. Figure 2 illustrates axes orientations.

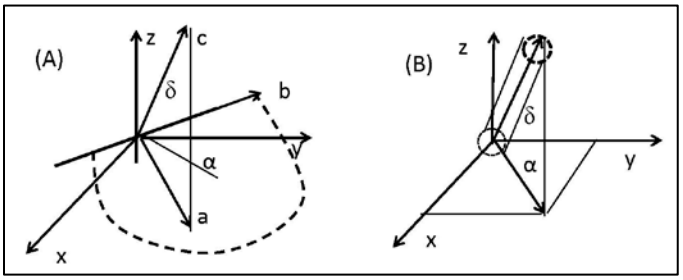

Figure 2. (A) Azimuth (α) and dip (δ) of anisotropy axes (abc) with respect to global axes (xyz) (B) Azimuth (α) and inclination (δ) of temporary hole axes (X'Y'Z') with respect to global axes (xyz).

An example of an anisotropic (orthotropic) input properties data file from a measurement campaign in a deep, hardrock mine situated in Precambrian meta-sediments is given in Figure 3. The first row contains Young's moduli and Poisson's ratios; the second row contains shear moduli and specific weights (when needed) and the third line contains angles. The first material is rock; the second material pertains to cement, and the third material is an HI.

1. ROCK N=2 a=down dip, b=normal, c=strike
   13.5E+06 7.2E+06 13.7E+06 0.23 0.15 0.22
   3.8E+06 3.9E+06 5.6E+06 .00 .00 0.00
   90.00 0.00 0.00 0.00
2. CEMENT
   0.50E+06 0.50E+06 0.50+06 0.40 0.40 0.40
   0.18E+06 0.18E+06 0.18E+06
   0.00 0.00 0.00 0.00
3. HI
   0.50E+06 0.50E+06 0.50+06 0.40 0.40 0.40
   0.18E+06 0.18E+06 0.18E+06
   0.00 0.00 0.00 0.00

Figure 3. An example of an input properties data file from engineering practice.

Step 2 Execution of the Finite Element Program

Execution of the finite element program is just a keystroke. In this regard, the finite element approach is intended to simulate actual HI use and is not simply a composite of numerical solutions to the

boundary value problems intended to approximate HI use. The difference is important, especially in consideration of axial strain. Results are delivery of gauge compliance and stiffness matrices [*C*] and [*S*], respectively, after successive applications of unit loads σ, that is, $\sigma_{xx} = \sigma$, $\sigma_{yy} = \sigma_{zz} = \tau_{yz} = \tau_{zx} = \tau_{xy} = 0$, then $\sigma_{yy} = \sigma$ and all other stresses are zero and so on. Application is to excavation of a hole in anisotropic rock followed by overcoring to depth, removal of the large overcored cylinder of rock and installation of an HI towards the hole bottom as in actual HI use. Each unit loading is followed by stress relief of the HI.

Figure 4 illustrates the finite element sequence simulating gauge use. The procedure requires two program passes for each unit load, one pass for hole excavation including old overcore and a second pass for gauge installation and final overcoring. There are 187,920 elements and 196,560 nodes in the mesh. External boundaries are far from the pilot hole and the overcore hole is far from the hole collar as seen in the figure. Accordingly, displacements at the external boundaries are fixed at zero in the normal direction. However, displacements of the internal face of the overcore are unrestricted as in practice and thus allow z-direction strain in the overcore and HI to occur during overcoring. Analysis is carried out in hole coordinates with origin at the bottom of the hole. The z-axis points out of the hole; x- and y- axes are in the usual orientation. Coordinates are right-handed, of course. Hole orientation in *isotropic* rock has no effect on the gauge stiffness matrix [S]. However, the computed stresses {σ} are relative to hole orientation. For example, Sxx relative to an East-West horizontal hole is the normal stress in the North-South direction when referred to compass coordinates. In general, a transformation of stress from borehole coordinates to compass coordinates or mine coordinates is required.

Step 3 In Situ Stress Computation

The third and last step is computation of the *in situ* stress $\{\sigma_o\} = [S]\{\varepsilon_g\}$. This computation can be carried in a spread sheet containing HI strains. In this regard, the effect of cement on HI performance was evaluated and found to be negligible provided the bond between HI and rock was secure and the cement stiffness was not smaller than the HI stiffness. Details are given in Appendix B Effect of Cement.

MINE EXAMPLES

Examples of stress measurement using HI gauges at four underground mines are described. Two mines are in Precambrian meta-sediments where precious metals are mined; a third mine is also in hardrock of Precambrian age and a fourth mine is in Cretaceous strata where coal was mined. Comparisons of inferred stress in isotropic and anisotropic cases illustrate the influence of anisotropy. Cement properties were considered equal to HI properties in the four mine examples following.

Homestake Mine

The first example is from stress measurements at the former Homestake Mine in the Northern Black Hills of South Dakota, U.S.A. The mine occurs in Precambrian meta-sediments where gold was found in the famous Homestake formation. The Poorman formation is below the Homestake and is the footwall; the hanging wall is the Ellison formation. The mine was developed to the 8000 ft level (2500 m) level and operated for over 100 years. After closure in 2006, the mine was reopened and redone as an underground research laboratory known as SURF (Sanford Underground Research Facility). Research facilities are now concentrated on the 4850 Level 1478 m (4,850 ft) below ground surface.

Stress measurement campaigns were conducted at the mine as part of a cooperative rock mechanics study between the Homestake Mining Company, the U.S. Bureau of Mines and the University of Utah (Johnson *et al* 1993). Other stress measurements were made prior to these efforts and led to formulas for normal stress as functions of depth (Pariseau 1985); shear stresses were an order of magnitude smaller than normal stresses. After conversion of the mine to a research laboratory, another campaign of stress measurements using HI Cells was conducted on the 4850 Level (Golder Associates 2010). In every case, the host rock was assumed to be isotropic and a standard data reduction scheme was used.

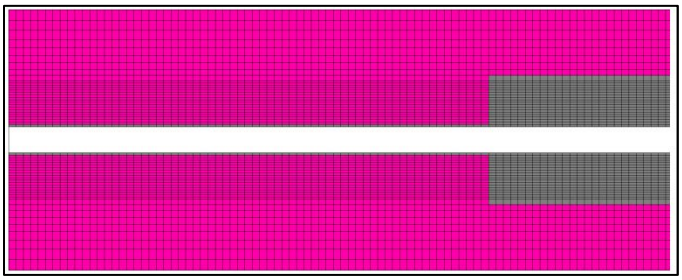

(A) Pilot hole and overcore prior to gauge installation. Grey=excavated elements. Hole diameter is d. Overcore diameter is D. Length of overcore is 1.5D. Length of hole from overcore bottom is 15.6d. D=146 mm (5.74 inches). d=38 mm (1.5 inches). 1 inch=25.4 mm.

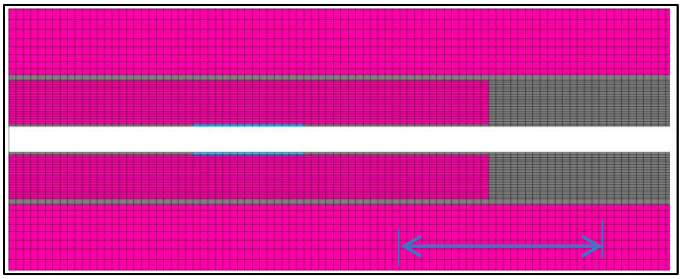

(B) After gauge installation (blue arrow) and overcoring. Grey=excavated elements. Gauge length blue) is 3.6d. Distances before and after gauge ends are 6d. The mesh is 823 mm (32.4 inches) long. Length of overcoring a gauge is 594 mm (23.4 inches)

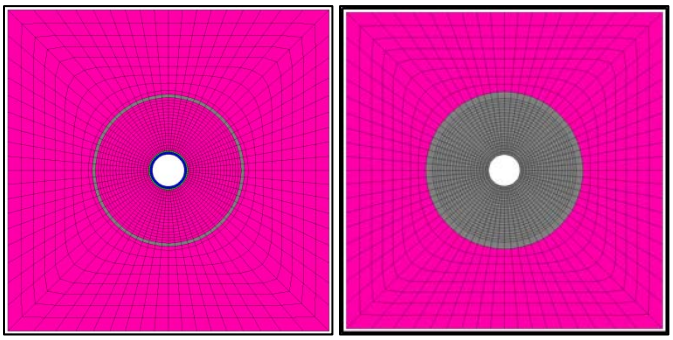

(a) (b)

(C) Cross-section: (a) pilot hole. (b) overcore. Section is square 322x322 mm (12.68x12.68 inches) or 8.5d square or 2.D square.

Figure 4 Schematic illustration of the finite element sequence simulating HI use. (A) hole cut and partial overcore, (B) HI installation and overcore completion, (C) cross-sections.

A comparison of results from finite element simulation (FEM), a measurement in amphibolite (GLD) and an independent data reduction (LAR) is given in Figure 5 where:

- FEM = finite element simulation
- GLD = Golder Associates 2010
- LAR = Larson 1992
- AVE = average.

In every case, Young's modulus for amphibolite[1] was 94.1 GPa and Poisson's ratio was 0.30. The epoxy HI Cell Young's modulus was 2.6 GPa and Poisson's ratio was 0.40. The results in the figure are referred to the finite element coordinate system where x=East,

[1] In the Yates member of the Poorman formation.

y=North and z=Up which is a standard orientation of Cartesian coordinates.

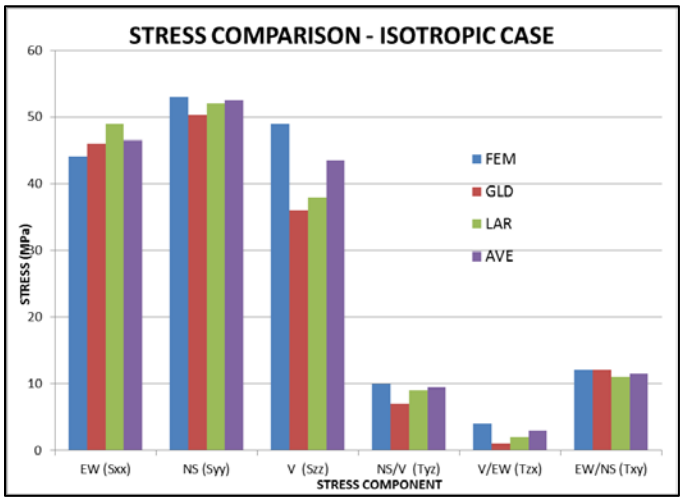

Figure 5. Comparisons of finite element (FEM), conventional (GLD), independent (LAR) and average stresses in the case of isotropy.

The results compare favorably in consideration of substantial variability on a meter scale between in-hole measurements and over tens of meters between-holes in the same rock type. "Substantial" implies differences of 23 to nearly 50 percent in the same stress component. Such variability is reasonably attributed to spatial variability of rock properties encountered in nature. Results in Figure 5 show differences in normal stress of roughly 10 percent about the average; percentage differences between the much smaller shear stresses are higher but less important. In this regard, averaging Cartesian stress components is a legitimate operation because the direction of action is the same for each component; averaging principal stresses is not meaningful. These results indicate proper functioning of the finite element approach.

The finite element data reduction process $\{\sigma_h\}=[S]\{\varepsilon_g\}$ may also be applied to the gauge strains $\{\varepsilon_g\}$ obtained from a post-measurement biaxial test. The result $\{\sigma_h\}$ should be the biaxial pressure applied to generate the recorded gauge strains. To be sure, the gauge stiffness matrix $[S]$ is the same matrix developed during application of unit loads in the finite element simulation. The result in case of the GLD data should be a stress state $\{\sigma_g\}$ = (25,25,0,0,0,0) in MPa. The actual result is $\{\sigma_g\}$ = (-28.5,-29,-2.5,-0.5,0.0,-0.2) where the negative sign is associated with load application rather than stress relief. This result indicates Young's modulus is high by 12 percent. Use of moduli 0.88 times the moduli used would reduce the measured stresses (GLD) by the same amount in consequence of linearity. This reduction would give a Young's modulus of 82.84 GPa (12.0×10^6). Interestingly, Pariseau and Trancynger (2012) report a Young's modulus of amphibolite of 84 GPa as an average of 30 tests

Principal stresses are of interest and are compared in Table 2. The data in the table were obtained from Cartesian stress data in Figure 5. A check on the processing was done by comparing Table 2 GLD results with principal stress results given in the Golder 2010 report. Magnitudes of the principal stresses are within 10 percent or so as were the normal stresses in Table 2. Directions are sensitive; azimuths (α) compare favorably, hole inclinations (δ) are less so, but principal directions are orthogonal in each case, as they should be.

Figure 6 is a photograph of the large overcore obtained during the measurement campaign on the 4850 Level of the Homestake site. Directional character of the core is clearly evident. Whether the evident anisotropy matters requires quantitative analysis.

Table 2. Principal stress comparison – isotropic rock.

*	S1	α	δ	S2	α	δ	S3	α	δ
FEM	67	37	30	43	242	56	35	130	14
GLD	61	38	14	39	296	37	32	145	49
LAR	64	38	17	42	297	31	34	153	54

*Compression is positive. Units=MPa. S1=major, S2=intermediate, S3=minor principal stress. α=azimuth clockwise from north, δ=inclination, +up.

Figure 6. Photograph of large overcore of amphibolite at the Homestake site on the 4850 Level.

Table 3. Poorman formation anisotropic elastic moduli.

*	Eaa	Ebb	Ecc	vab	vbc	vca	Gab	Gbc	Gca
GPa	93.1	94.5	49.6	0.22	0.29	0.12	38.6	26.2	26.9

Note: vab / Eaa = vba / Ebb and so forth, in consideration of symmetry.

In case of anisotropic rock, the finite element approach is the only approach available for quantitative analysis of HI Cell strain measurements. Elastic properties of the anisotropic Poorman formation are given in Table 3[2] where E=Young's moduli, v=Poisson's ratios, and G=shear moduli. The direction a=down dip of foliation, b=is on strike, and c=normal to foliation. The ab plane is the plane of foliation. Young's modulus normal to foliation is roughly one half the moduli parallel to foliation. The Poorman formation, indeed, is highly foliated and shows the greatest differences in moduli of the three major formations at the mine. The ratio of maximum to minimum Young's moduli is 1.9. In case of the weakly anisotropic Homestake formation, the ratio of maximum to minimum moduli is 1.4. Details are given in Pariseau *et al* (1995).

A comparison of stresses in assumed isotropic rock with anisotropic rock (Poorman , phyllite) based on finite element simulation is given in Figure 7. The plane of foliation is flat with the a-axis of anisotropy parallel to the global x=E-axis (east) with y=N=north and z=U=Up. The results in the figure are for a measurement hole that crosses the foliation plane at an angle (azimuth=-63 deg, inclination up +38 deg). The strains are from measurements reported in Golder 2010 (GLD). Data were reduced using the finite element approach (FEM), that is $\{\sigma_o\}=[S_o]\{\varepsilon_g\}$; $\{\sigma_o\}$ =(Sxx,,.,Txy). Moduli Eaa and Ebb of the Poorman formation and E of the amphibolite are comparable; Ecc of the Poorman is about half the value of Eaa and

[2] The b and c axes in Table 3 are interchanged from Figure 3.

Ebb of the Poorman formation. These results indicate a significant effect of anisotropy in this example comparison based on measured HI strains. Magnitudes and algebraic signs of the stresses are consistent, but the normal stresses in the isotropic case are noticeably larger while the magnitudes of shear stresses are comparable.

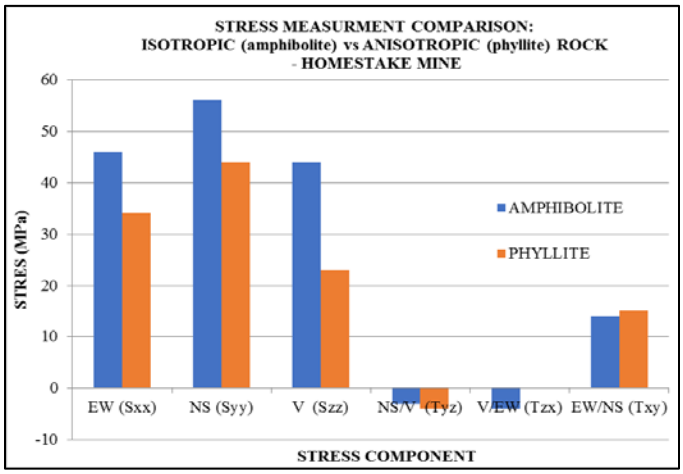

Figure 7. Stress measurement comparisons between isotropic and anisotropic rock.

Measurements using HI were also done on the 3650 Level of the mine in conjunction with a study of shaft pillar mining (Johnson *et al* 1993). Five successful HI measurements were made in the weakly anisotropic Homestake formation. Measurement data were reduced assuming isotropy with a Young's modulus of 45 GPa and a Poisson's ratio of 0.2. Strains from sample S2H1C1 (site 2, hole 1,cell 1) were estimated and then used to compute stresses *in situ* using the finite element approach (FEM) in the isotropic case and in the case of anisotropic Homestake formation properties shown in Table 4. The ratio of maximum to minimum Young's moduli in the Homestake formation is 1.42. Anisotropy in the Homestake formation is thus relatively weak compared with the Poorman anisotropy.

Table 4. Homestake formation anisotropic elastic moduli.

*	Eaa	Ebb	Ecc	vab	vbc	vca	Gab	Gbc	Gca
GPa	88.3	62.1	64.1	0.27	0.18	0.10	26.9	33.1	29.7

Note: vab / Eaa = vba / Ebb and so forth, in consideration of symmetry.

A comparison of results is given in Figure 8. The results in the figure clearly indicate a significant effect of anisotropy even when the anisotropy is relatively weak. Of course, an increase in the isotropic Young's modulus would change the results. The isotropic moduli used in this comparison are the same used in the reference that supplied the strain measurements (Johnson *et al* 1993).

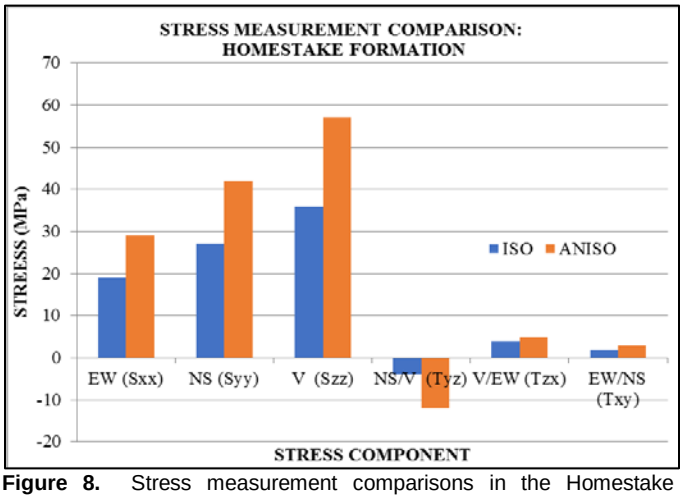

Figure 8. Stress measurement comparisons in the Homestake formation.

Lucky Friday Mine

The Lucky Friday Mine is located in northern Idaho in the famous Coeur d'Alene mining district. The mine has been in operation for more than75 years and produces silver, lead and zinc concentrates. A recent shaft sinking now extends to 2,713 m below ground surface. Precambrian meta-sediments include quartzite, argillite and phyllite with gradations, for example, of pure quartzite to argillaceous quartzite (Slaughter 1968). Numerous stress measurements were made on the 5300 Level using doorstopper stress gauges as described in detail by Whyatt *et al* (1995a, 1995b, 1995c, 1995d).

Transformation of principal stress to xyz (East, North, Up) coordinates results in *in situ* stress: Sxx= 114 Syy=74 Szz=89 Tyz=5 Tzx=30 Txy=7 MPa associated with a measurement in Hole 4 on the 5300 Level. Quartzites dip 60 deg and bear north at the site. A Young's modulus of 69 GPa and a Poisson's ratio of 0.1 were used in the study (Whyatt *et al* Part 2). These data may be used to convert doorstopper measurements to HI measurements via the *in situ* stress. At the outset $\{\sigma_g\}=[T]\{\sigma_o\}$, then in the finite element approach $\{\varepsilon_g\}=[C]\{\sigma_g\}$ where the subscript *g* indicates *gauge* and where $\{\varepsilon_g\}$ are nine HI strains. As before $\{\sigma_o\}=[S_o]\{\varepsilon_g\}$ where $\{\sigma_o\}$ are the six *in situ* stresses referred to the global xyz (ENU) axes. The process is circular but the computed HI strains are useful provided the input and output $\{\sigma_g\}$ and $\{\sigma_o\}$ are in reasonable agreement. Usefulness is in the anisotropic case. Table 5 contains a comparison of the input and output of these stresses and shows the finite element results are in quite reasonable agreement.

Table 5. Input and output gauge and global stress (MPa).

Gauge Input	Gauge output	Global output	Global input
72.4	72.4	113.7	113.7
86.4	86.3	73.7	73.8
117.8	117.8	89.2	89.1
29.1	29.2	4.9	4.8
0.4	0.4	30.1	30.0
-0.2	-0.2	7.3	7.8

Only one finite element computation is needed in case of anisotropy and that is the computation of unit load matrices [*S*] and [S_o]. Recall $\{\sigma_g\}=[S]\{\varepsilon_g\}$ and $\{\sigma_o\}=[S_o]\{\varepsilon_g\}$. A comparison of results based on the same HI strains $\{\varepsilon_g\}$ then allows for assessment of the importance of anisotropy at the measurement site. Elastic properties for rock in the anisotropic case are shown in Table 6. The ratio of maximum to minimum Young's moduli is 2.74. The intermediate value of Young's modulus Ea is close to the isotropic Young's modulus of 69 GPa.

Table 6. Lucky Friday Mine anisotropic elastic moduli.

Ea Eb Ec GPa	Ga Gb Gc GPa	vab vbc vca -
69.8 91.7 33.6	36.8 1.2 20.9	0.09 0.11 .13

Figure 9 compares stresses inferred from HI strains in the isotropic and anisotropic case using the finite element approach (FEM). In the anisotropic rock case, results differ greatly from the isotropic rock case. Clearly, anisotropy matters in this example.

Stillwater Mine

The Stillwater Mine is located in south central Montana in the famous Stillwater complex where palladium and platinum are of interest. The Stillwater complex is an ultramafic intrusion that has great horizontal continuity (over 25 miles) and considerable depth. The complex dips steeply from 45 deg to 70 degrees. Original interest in the Stillwater complex was for chromite (Johnston 1968).

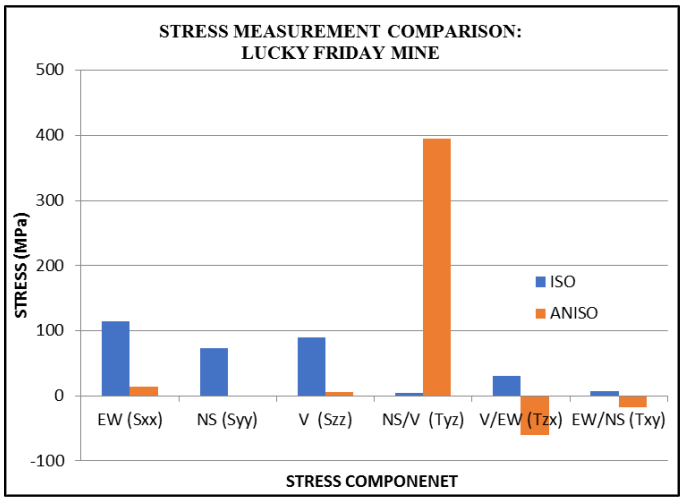

Figure 9. Stress measurement comparisons. Lucky Friday Mine, 5300 Level.

Stress measurements at the Stillwater Mine (Johnson *et al* 2003) were done using Australian Hollow Inclusion Cells (HI's). Reported data were sufficient to exercise the finite element program for estimating stress *in situ* from HI strain gauge data. Rock was considered isotropic at the Stillwater Mine for data reduction reported and in finite element analysis. A second finite element analysis was done assuming the same HI strains were obtained in anisotropic rock. The purpose was to assess importance of anisotropy relative to the isotropic case. Rock properties in the isotropic case were E=48. 3 GPa and v=0.29. Anisotropic properties assumed a vertical transverse isotropic rock with a bearing such that the gauge hole was parallel to one of the axes of anisotropy (an in-plane axis). Anisotropic properties are shown in Table 7.

Table 7 Stillwater Mine aistropic elastic moduli.

Ea Eb Ec GPa	Gab Gbc Gca GPa	vab vbc vca -
48.3 96.6 96.6	18.6 37.2 37.2	0.29 0.31 0.31

Figure 10 compares results in the case of the "Valley" measurement at the mine. The reported Stillwater valley stress (STW blue) and the finite element result (FEM/ISO red) are within about 10 percent and thus compare reasonably well. In the anisotropic case (FEM/ANI grey) results are very different from the two isotropic cases. Anisotropy thus makes a substantial difference in this example.

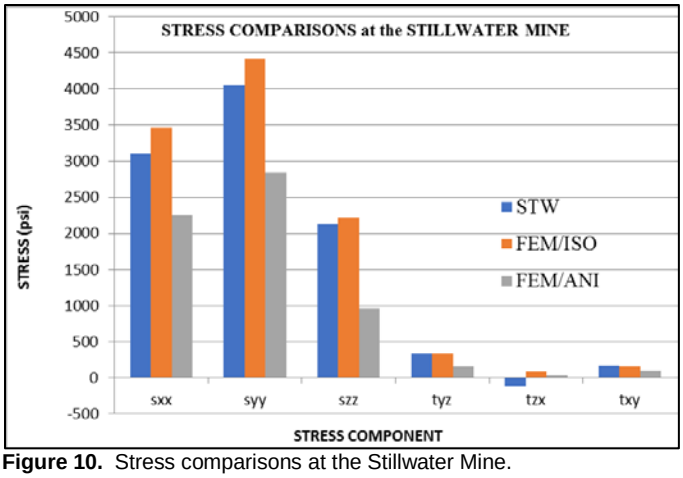

Figure 10. Stress comparisons at the Stillwater Mine.

Beaver Creek Mine

The Beaver Creek No. 2 Mine is in the Wasatch Plateau coal field of central Utah, U.S.A. Strata of Upper Cretaceous age include sandstones, siltstones, shales and some limestone (Mining Plan Decision Document 1984). The seam of interest is the Castle Gate "A". Depth is 229 m at most. Mining height is 2.4 m. The immediate roof is 0.3 m of sandstone; a grey siltstone overlies the sandstone roof. Floor is the Starpoint sandstone. The first 9-gauge HI was installed 3.8 m in a vertical roof hole (Larson 1987) in siltstone. Although gauge readings were obtained and several additional HI were installed and overcored, operational difficulties precluded successful stress measurement.

However, horizontal stresses were measured using the U.S. Bureau of Mines borehole deformation gauge in a vertical hole. Results indicated principal stresses: σ_H = 0.97 MPa, S42E and σ_h =0.41 Mpa, N48W. The vertical stress was estimated to be 5.2 Mpa. A Young's modulus of 11.9 Gpa and a Poisson's ratio of 0.14 were assigned to the measurement site. These properties allow calculation of what HI strain readings would be were these stresses inferred from HI measurement data. In global ENU coordinates, the *in situ* stresses are: : Sxx=0.66 Syy=0.72 Szz=5.2 Tyz=0 Tzx=0 Txy=-0.28 Mpa which are the same for a vertical gauge hole. This state of stress is noteworthy for lack of vertical shear stress.

With calculated HI readings at hand, the importance of anisotropy can be evaluated using the comparison technique applied in the previous example. In this regard, the global state of stress and the local or gauge stress state are the same in case of a vertical hole. Because the vertical shear stresses are zero, a division by zero in the finite element procedure occurs. A simple remedy is to specify small vertical shear stresses, say, 6.9 Pa. This remedy should also be applied in an unusual case of zero normal stress. Strata properties in the anisotropic case are given in Table 8. Comparison of isotropic with anisotropic results is given in Figure 11. Again, anisotropy matters in stress measurement data reduction.

Table 8 Beaver Creek Mine anisotropic elastic moduli.

Ea Eb Ec GPa	Gab Gbc Gca GPa	vab vbc vca -
11.9 5.9 5.9	5.2 2.6 2.6	0.14 0.10 0.10

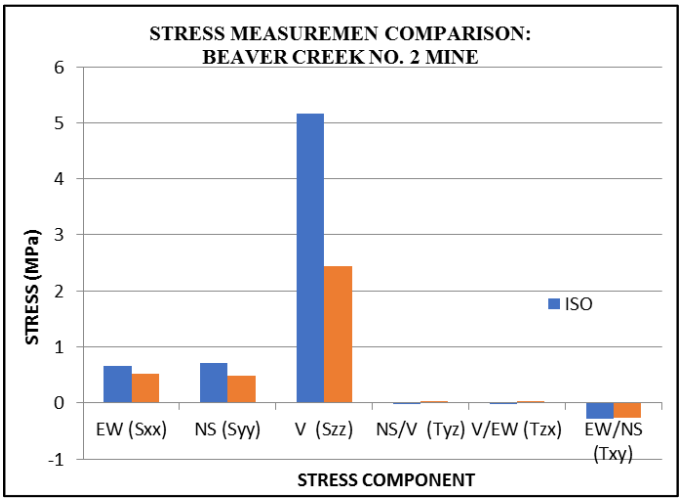

Figure 11. Stress measurement comparisons at the Beaver Creek Mine.

FINITE ELEMENT PROCEDURE - MONITORING

Development of a finite element procedure (FEP) for stress gauge data reduction follows from a series of numerical experiments on a three dimensional test block that indicate suitability of plane strain analysis for mine application to bore stress meters and borehole deformation gauges. Applications to borehole stress meters and borehole deformation gauges demonstrate the ease of use and effectiveness of the finite element approach. Synthetic borehole diameter change data developed from prior stress measurements and borehole diameter change measurements from two, deep underground hardrock mines in Precambrian meta-sediments are used in the

demonstration. The proprietary program UT3 is used in the present work. This program has been in use for many years in application to a wide range of rock mechanics problems such as mine subsidence (Pariseau and Voight 1970), slope stability (Pariseau and Stout 1972, Pariseau, Shmelter and Sheik 1997), stope stability (Pariseau et al 1984, Pariseau 1994), shaft stability (Pariseau, Johnson and Orr 1990), and more recently to foundations on jointed rock (Pariseau 2017). The program has several options beyond purely elastic analyses and has been repeatedly benchmarked against known and other numerical solutions. One-way coupling with fluid flow is allowed in case of wet ground and thermal stresses are allowed when of importance such as in geological containment of high-level radioactive waste. However, any finite element program capable of simple stress analysis in elastic solids could be used to implement the procedure for stress monitoring described here, and for stress measurement for that matter, e.g., Abaqus or Elfin, or the finite difference program FLAC3D, *provided* anisotropic rock is allowed.

A borehole stress meter (BSM) is essentially a hollow steel cylinder with an outside diameter of 5.72 cms, an inside diameter of 3.30 cms, and is about 25.4 cms or so long. A block of rock 152.5 cms or so on edge would allow experimental testing of a BSM in central hole through the block. Such a test would begin with an initial set of forces uniformly distributed over the faces of the block. These forces would correspond to stresses

$$\{\sigma^o(t_o)\} = (\sigma^o_{xx}, \sigma^o_{yy}, \tau^o_{xy}, \sigma^o_{zz}, \tau^o_{zy}, \tau^o_{zx}) \tag{6}$$

Drilling a hole induces stress change in the vicinity of the hole:

$$\{\Delta\sigma(t_o)\} \tag{7}$$

After drilling the hole the stresses at time t_o are

$$\{\sigma(t_o)\} = \{\sigma^o(t_o)\} + \{\Delta\sigma(t_o)\} \tag{8}$$

Because stress change diminishes rapidly away from the hole wall, the stresses several diameters away from the hole wall are close to the prehole stresses (6). If a BSM is installed in the hole shortly after drilling the hole, the stress field is still given by (8).

However, if the forces on the test block faces are changed at some later time *t* after gauge installation, then the new forces correspond to stresses

$$\{\sigma^o(t)\} = (\sigma^o_{xx}, \sigma^o_{yy}, \tau^o_{xy}, \sigma^o_{zz}, \tau^o_{zy}, \tau^o_{zx}) \tag{9}$$

These stresses are those that would be present in the test block without any hole or gauge. The stress field is given by

$$\{\sigma(t)\} = \{\sigma^o(t)\} + \{\Delta\sigma(t)\} \tag{10}$$

where the last term on the right-hand side of (10) is the induced stress change. Again, the stress change induced by the force change diminishes rapidly from the hole wall on either side of the gauge and beyond the gauge-wall interface.

At the faces of the test block, the change in applied forces is associated with the change prehole stresses. Thus,

$$\{\sigma(t) - \sigma(t_o)\} = \{\sigma^o(t)\} - \{\sigma^o(t_o)\} \tag{11}$$

A boundary value problem that describes the experimental test would involve tractions on the external faces of the test block. The hole wall and the inner surface of the gauge would be traction free. The applied tractions are changes

$$\Delta T_i = \Delta\sigma_{ji} n_j \qquad (i, j = 1, 2, 3) \tag{12}$$

where subscript notation and summation convention are used and n_j are components of an outward unit normal vector to the surface point where the tractions are computed.

A BSM is assumed to be in elastic rock, so the response to load is also elastic and superposition applies. The finite element analysis of the test block experiment is also elastic and, importantly, linear. These observations allow one to define a new stiffness [*k*] that relates displacement change at a given node to the applied stress. Thus,

$$\{\Delta\sigma\} = [k]\{\Delta\delta\} \tag{13}$$

where the left-hand side is a vector of stress change applied at the test block faces. This change corresponds to a change in the background or prehole stress, that is, in the stress *in situ*. After a series of uniaxial loads are applied to a mesh containing a BSM, the result allows computation of the stiffness matrix [*k*] in (8).

However, the computation of [*k*] is not unique. This feature of FEP is not discussed by Corthesy et al (2016). The reason is in the boundary conditions used in the series of forward finite element computations. For example, one may use a block model containing a gauge rather than a plane strain (slab) model. A block model is shown in Figure 12. The model extends 10 hole diameters from the origin to the mesh sides, top and bottom. Length of the mesh is also 10 times hole diameter. Gauge length is specified to be 3.3 times hole diameter (19.05 cms) in the model. The model is symmetric about the back plane that passes through the center of the gauge normal to the hole axis, so only a half gauge appears in the figure. Figure 13 shows the mesh in long section parallel to the hole axis. The blue elements represent a half-length gauge; gray elements are air elements (excavated). A block model is responsive to axial stress change unlike a slab model (plane strain) where an axial stress (strain) correction is needed.

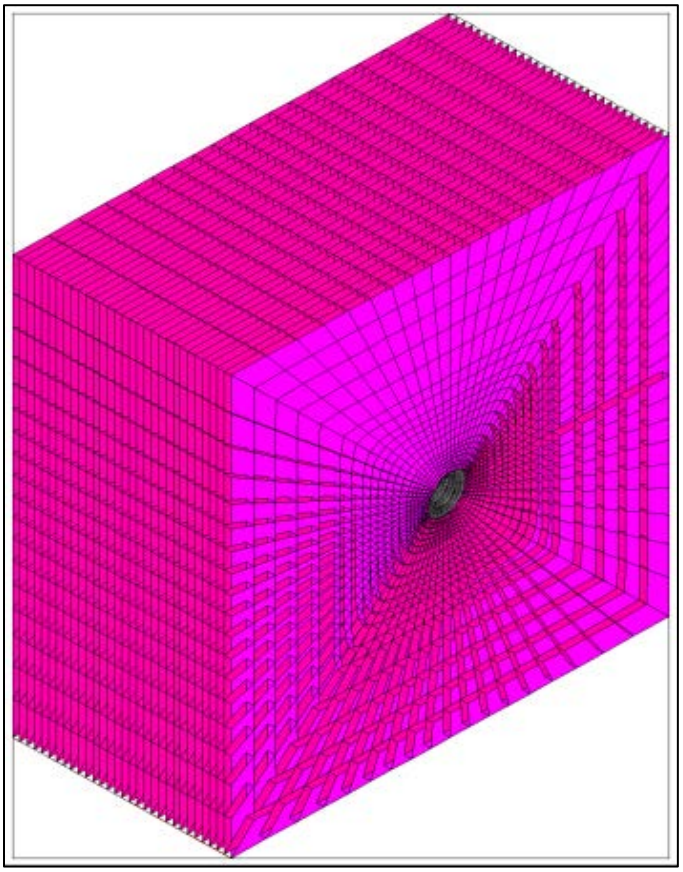

Figure 12. Block finite element mesh containing a borehole stress meter.

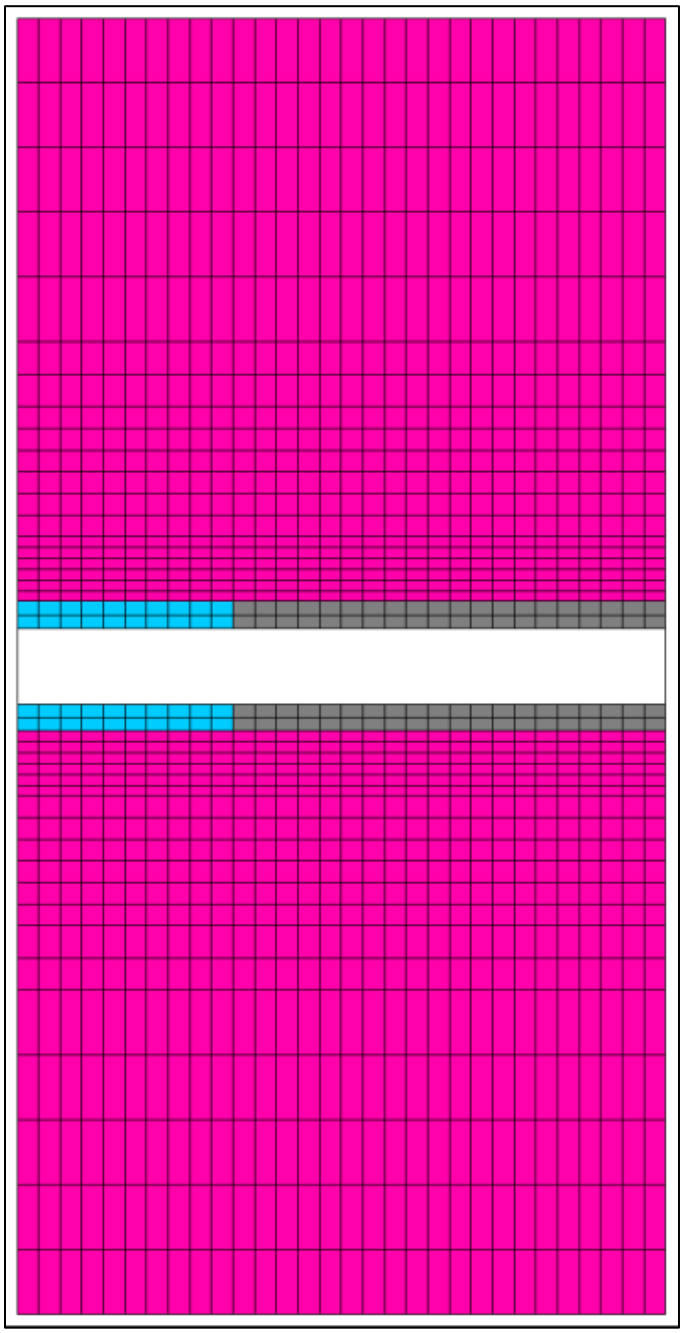

Figure 13. Long section through the block model center. Gauge elements are blue. Air elements are grey.

The top, bottom and sides of the block are sufficiently far from the gauge to have a negligible effect on stress, strain and displacement changes near the gauge. The reason is the rapid decrease of induced changes with distance from the gauge hole. Thus, the outer boundaries may be fixed at zero displacement or at zero stress except at the side where forces are applied. Fixed and free boundary conditions are illustrated in Figure 14. Strictly, displacement and stress change approach zero only as the distance from the hole wall increases indefinitely, that is, mathematically approaches infinity. The block model faces are within a finite distance from the hole, so there are differences in hole wall displacement associated with different boundary conditions. However, hole wall diameter changes are not so different.

Table 9 compares hole wall displacements under various boundary conditions for the block and slab models. The data were obtained by loading in the x-direction only. Displacements in the table are at an interface node on the x-axis (horizontal axis). Differences in the table are noticeable. Vertical displacements occur when the mesh bottom is fixed while the top is free, although there should be no vertical displacement at the test node on the x-axis in these analyses. However, displacements in a finite element analysis are not absolute but rather are relative. The relative y-displacement is zero. A change in borehole wall diameter is a relative displacement between points separated by 180 degrees along the hole wall. The sum of radial displacements (outward is positive) between two such opposing points is a change in borehole diameter and not simply twice the radial displacement at any one point at the borehole wall.

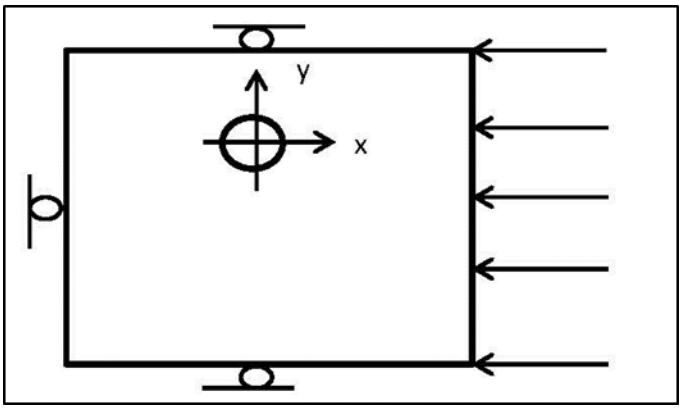

(A) Uniaxial load, fixed side (roller), fixed top and bottom (roller).

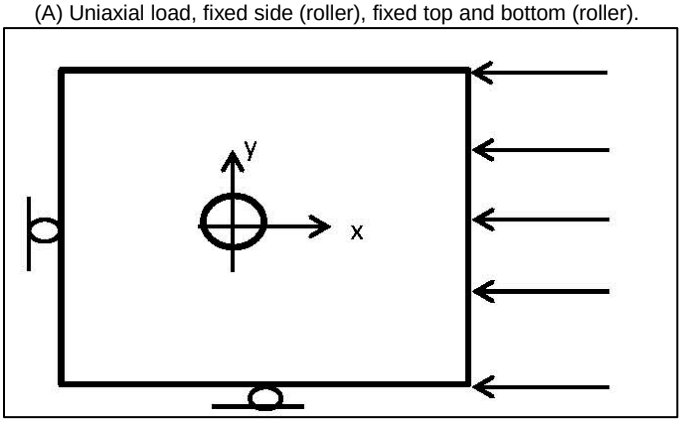

(B) Uniaxial load, fixed side (roller), top free (no roller), bottom fixed (roller)

Figure 14 Fixed and free boundary conditions under uniaxial load. In slab and block models the faces parallel to the plane of the page could also be fixed or free. Arrows denote a uniformly distributed load; rollers indicate fixity normal to a face.

Table 9. Borehole wall displacements under different boundary conditions.

Displacements Model	Horizontal (mm)	Vertical (mm)	Diameter Change (mm)	Boundary Code
Slab 1	-0.0027432	0	-0.00552196	0 0 1 1 1 1
Slab 2	-0.0515366	0.0233934	-0.00801624	1 0 1 0 1 1
Slab 3	-0.0575818	0.017653	-0.0089662	1 0 1 0 1 0
Slab 4	-0.0515366	0	-0.0802005	1 0 0 0 1 1
Slab 5	-0.0387604	0	-0.0054864	1 0 1 1 1 1
Block 1	-0.0586994	0.0180848	-0.0090551	1 0 1 0 1 0
Block 2	-0.039624	0	-0.00569722	1 0 1 1 1 1
Block 3	-0.0396748	0	-0.00569468	1 0 1 1 1 1
Block 4	-0.0387604	0	-0.0054864	1 0 1 1 1 1

* 1=zero displacement (rollered), 0=zero stress (free)

Slab 1 and Slab 5 models are essentially the same models and give nearly the same diameter change at the test node. Slabs 2, 3 and 4 are also the same models and give the same diameter change at the test node. The diameter changes in these three models are larger

than the previous slab models because of the unrestricted motion in the y-direction. Thus, the slab model results show larger displacements when a face opposite a fixed face is free, a larger diameter change occurs than when both opposing faces are fixed.

The Block 1 model with opposing faces fixed and free also shows a larger diameter change than the Block 2 model with opposing faces fixed, excluding the loaded and opposing face as in the slab models.

The Block 3 model has an open hole length beyond the gauge that is twice the length in case of the Block 2 model. Results are nearly the same indicating the open hole length in the model is not a factor in the diameter changes. The Block 4 model has a gauge over the entire hole length and is thus comparable to the Slab 5 model (and Slab 1 model). These models are in close agreement as they should be.

The slab models have 1,512 elements and 3,168 nodes. The block models have 45,360 elements and 49,104 nodes, except the Block 3 model that has 75,600 elements and 80,784 nodes. Block model run times are 28 minutes; slab model run times are much less, about 1 minute. Because results are comparable, the slab model is preferred.

However, there remains a question about the open hole beyond gauge ends. If the hole is grouted and not open, there will be an unknown influence on hole diameter change in response to a given change in the background stress. Further numerical experimentation could quantify such an effect.

An axial compression decreases hole wall diameter D, and therefore increases stiffness [*k*] relative to the case of no axial compression. Consequently, neglect of such a correction is on the optimistic side with a smaller stress change than with a correction when the axial stress change is a compressive stress change.

In case the hole is grouted after gauge installation, somewhat different results are expected. In this regard, no existing data reduction procedure allows for the finite length of a gauge or the condition of the hole beyond the gauge.

There is an alternative to the finite element procedure requiring external loading and modification of boundary conditions for each uniaxial load (SXX, SYY, TXY) that does not require modification of external boundary conditions but rather uses the same boundary conditions for each of the three loads leading to the desired stiffness matrix. The procedure is to simply excavate a circular opening in initially stressed ground with gauge already present. This procedure uses fixed external boundaries for each of the three initial stress states (SXX, SYY, TXY).

Overall results of the numerical experiments indicate a plane strain (slab) model is the model of choice. This model gives the smallest diameter change for a given load and thus gives the stiffest response. Stress change associated with measured diameter change is greater in case of stiffer rock models. A relatively stiff model is therefore conservative.

APPLICATION TO BOREHOLE STRESS METERS

A Geokon[3] Model 4350 Biaxial Stressmeter is an example of a BSM. This gauge is a hollow steel cylinder that is cemented in a borehole. This gauge responds to changes in the diameter of a borehole at three points spaced 60 degrees around gauge circumference. No theoretical solution exists in case of anisotropic rock which is more the rule than the exception in deep, hardrock mines such as the Lucky Friday Mine (LFM) in the famous Coeur d'Alene mining district of northern Idaho, USA, and the former Homestake Mine (HSM) in the northern Black Hills of South Dakota, USA. Both are in Precambrian meta-sediments, quartzites, siltites, phyllites and schists, which show directional characteristics and are measurably anisotropic. Visual evidence of anisotropic effects is often observed between rock bolting requirements in drifts along the "grain" and crosscuts across the "grain". Mines in strata bound ore bodies and in soft rock mines also often show rock properties that are directional, say, parallel and perpendicular to bedding.

[3] Mention of any commercial product is not intended as an official endorsement.

PROCEDURE

The procedure for using the finite element approach is straightforward. There are three steps necessary. The **first** step is to prepare a material properties file for rock and gauge including orientation data for rock anisotropy and gauge hole orientation. The **second** step is to prepare a runstream file for the finite element program and then to execute the program. The **third** step is to copy the stiffness matrix from a finite element output file into a spreadsheet such as Excel that contains BSM data of interest, specifically, displacement changes along the three gauge diameters (0-60-120). A simple matrix multiplication $\{\Delta\sigma\} = [k]\{\Delta\delta\}$ gives the associated stress changes. The process is repeated for each gauge at the mine of interest. Several examples illustrate the procedure.

The material properties file has the form shown in Figure 15 and is a text file with a name and extension: *name.txt*. The file contains properties for rock and gauge. The first line is a name of the rock containing the gauge and a reminder of rock anisotropy directions: *a* is down dip, *b* is on strike, and *c* is normal to the *ab* plane. Anisotropy up to orthotropy is allowed. Gneiss is an example of a rock type that would be orthotropic. Schists and phyllites may also be orthotropic. Shales and laminated sandstones may be transversely isotropic with two distinct material directions, parallel and perpendicular to bedding. The next line contains three Young's moduli and three Poisson's ratios: E_{ab}, E_{bc}, E_{ca}, ν_{ab}, ν_{bc}, ν_{ca}. The third line contains three shear moduli: G_{ab}, G_{bc}, G_{ca}. Units of Young's moduli and shear moduli are *psi*. Poisson's ratios are dimensionless. These properties are referred to the axes of anisotropy as indicated by the subscripts. The fourth and last line contains two pair of numbers. The first pair gives the dip direction or azimuth (α) and dip (δ) of the *a*-axis of anisotropy. The strike direction is equal to the dip direction less 90 degrees. The dip is down from the horizontal and ranges from 0 to 90 degrees. A vertical formation that strikes due north has α=90 degrees and δ=90 degrees. The second pair of numbers gives the gauge hole orientation as an azimuth (α) and an inclination (δ). A vertical up-hole has α=0 degrees and δ=90 degrees. As usual, azimuth is measured positive clockwise from north. However, hole inclination is positive for an up-hole, that is, one is looking upwards when looking into the hole collar. Gauge material is isotropic and orientation is of no consequence. Entering zeroes saves computer time because axes rotation is not needed. Figures 16 and 17 illustrate the meaning of the orientation parameters for rock and hole. Figure 18 shows the final axes orientation for a BSM.

```
1     --(1) LUCKY FRIDAY WALL ROCK  a=downdip, b=strike, c=normal
      10.12E+06 13.32E+06  4.87E+06     0.09     0.11     0.13
      5.34E+06  3.07E+06  3.03E+06
      90.0     90.0     0.0     90.0
2     --(2) STEEL GAUGE
      30.0E+06  30.0E+06   30.0+06     0.33     0.33     0.33
      11.28E+06 11.28E+06 11.28E+06
      0.00     0.00     0.00     0.00
```

Figure 15. A material properties file for a BSM finite element analysis.

Although a free format is used during a finite element run, alignment of the numbers in the material properties file is recommended and spaces between numbers are required. Gauge and hole geometry are automatically taken into account.

All stresses, strains and displacements are referred to the coordinate axes shown in Figure 7 regardless of hole orientation. In this regard, tension is positive, compression negative. Positive displacements are in the positive coordinate directions. Displacement in the radial r-direction is positive outwards. A diameter change is the sum of radial displacements at an angular spacing of 180 degrees. If there is material properties symmetry as there would be in case of isotropy and symmetry of applied stress, then the change in diameter at any point along the hole wall is just twice the radial displacement at that point, but only in this special case.

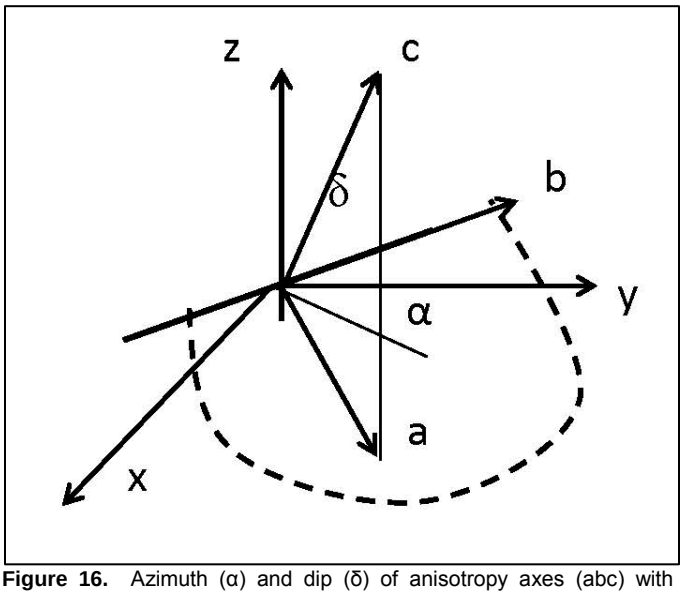

Figure 16. Azimuth (α) and dip (δ) of anisotropy axes (abc) with respect to global axes (xyz).

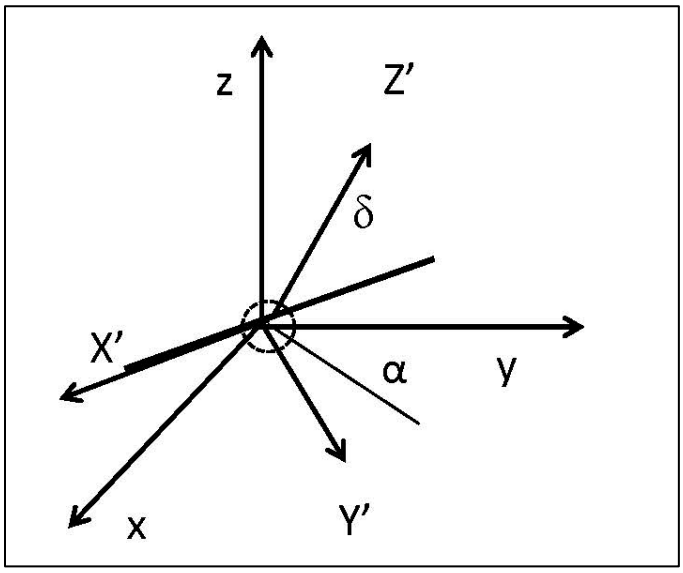

Figure 17. Azimuth (α) and inclination (δ) of temporary hole axes (X'Y'Z') with respect to global axes (xyz).

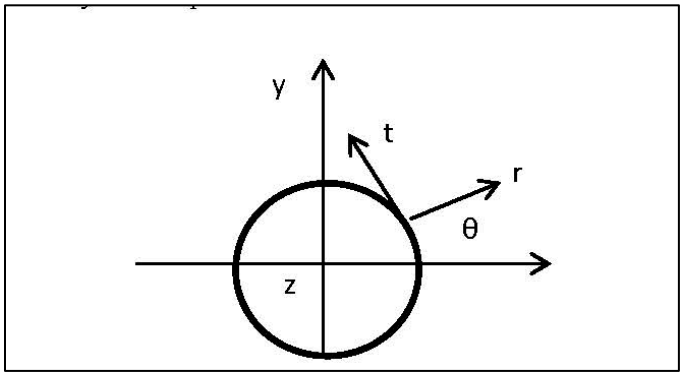

Figure 18. Sketch showing coordinate axes in a final, standard position relative to a borehole. The view is at a hole collar looking into the hole. Axis z points out of the hole.

A runstream file is shown in Figure 19. This file is also a text file: *filename.txt.* There are only three lines to edit in this file. The first line is a title line that is handy for identification. The second line is the name of the text file containing the material properties (Figure 15). The next four lines are file names that should not be changed. These files are generated automatically from the start of an analysis. They identify finite element files for elements, coordinates, cut elements, and boundary specifications. The last line is a prefix used to label output files from the run. Output files are a file that echoes some of the input data and a file containing compliance and stiffness matrices for subsequent data reduction.

```
vert HOLE BSM isotropic rock with gauge LFM
aniso5.txt
relms
rcrds
rctel
rnsps
LFM
```

Figure 19. A runstream file for computing a BSM compliance and stiffness matrices.

Clicking on the executable program BSM.exe results in a screen request for a runstream file name. After typing in the runstream file name, a run begins. However, if the run is a repeated try or if the output prefix has been used previously, a question is asked whether the file should be overwritten or a new file prefix is desired. After responding, the run continues. Run information is written to the screen. Completion is in a matter of seconds.

Output files here include a runstream echo file LFM and a file BSM containing compliance matrix [*c*] and stiffness matrix [*k*] which are mutual inverses, so the product should be a 3x3 diagonal matrix with ones on the diagonal. Figure 20 is a BSM output file where CB(3,3)=[*c*] and BC(3,3)=[*k*]. The product is [I], the identity matrix. The diagonal elements of [I] are ones as they should be; the off-diagonal elements are very small numbers relative to the diagonal ones and are zeroes as a practical matter. This matrix product provides a check on the compliance and stiffness matrices.

```
compliance matrix CB(3,3)
 -0.911635E-07  0.140890E-06  0.119011E-12
  0.829320E-07 -0.329388E-07  0.199667E-06
  0.829320E-07 -0.329388E-07 -0.199667E-06
   inverse = stiffness BC(3,3)
  0.379415E+07  0.811441E+07  0.811441E+07
  0.955277E+07  0.525047E+07  0.525047E+07
  0.128113E+01  0.250417E+07 -0.250417E+07
   matrix product [CB]*[BC]=[I]?
  0.100000E+01  0.000000E+00 -0.596047E-07
 -0.422250E-07  0.100000E+01  0.000000E+00
  0.422250E-07  0.596046E-07  0.100000E+01
```

Figure 20. A BSM output file.

LFM EXAMPLES

The Lucky Friday Mine is a deep vein mine in Precambrian meta-sediments. Silver, lead, zinc vein widths range to 20 ft. Recent completion of a #4 Shaft extends the mine to 2,926 m below ground surface. Estimates of *in situ* stress at the mine after extensive review of measurement data by Whyatt et al(1995) are used to generate borehole diameter changes associated with a borehole stress meter. These data are synthetic because they are generated in a forward computation of stress about a fictitious BSM. However, as part of an extensive research effort to improve mine safety, ten borehole stress meters were installed in holes collared on the 5550 Level. The data from these gauges is real, of course. Both sets of data provide examples of the new FEP for data reduction.

The stress measurement review leads to the *in situ* stress formulas:

$$\begin{gathered} \text{Sns=0.57, Sew=0.50, Sv=0.36,} \\ \text{Tns/ew=-0.14, Tns/v=0.02, Tew/v=0.09} \end{gathered} \qquad (14)$$

Units are kPa per m of depth; S=normal stress, T=shear stress, ew=east-west, ns=north-south, v=vertical. Depth at the collar of BSM1

(borehole stress meter 1) hole is 1,676 m. Thus the *in situ* normal stress are

$$\sigma_{ns}^{o} = 94.8,\ \sigma_{ew}^{o} = 83.4,\ \sigma_{v}^{o} = 60.7 \text{ MPa} \qquad (15)$$

with allowance for round-off.

Table 10 shows the isotropic rock and gauge properties data; Table 11 shows the anisotropic rock properties from Johnson et al (2016). As a reminder, the directions *a, b, c* are down dip, on strike and normal to the dipping ab plane, respectively. Interestingly, Young's modulus normal to the foliation is much less than the moduli parallel to the foliation. Shear moduli across the foliation are less than parallel to the foliation as one might expect.

Table 10 Rock and gauge properties (isotropic analyses).

PROPERTY MATERIAL	E GPa	G GPa	v -
ISOTROPIC ROCK	36.8	13.8	0.33
STEEL GAUGE	206.90	77.2	0.33

E=Young's modulus, G=shear modulus, v=Poisson's ratio

Table 11 Rock properties for anisotropic rock

PROPERTY MATERIAL	Ea Eb Ec GPa	Gab Gbc Gca GPa	vab vbc vca -
ANISOTROPIC ROCK	10.12 13.32 4.87	5.34 3.07 3.03	0.09 0.11 0.13

Results of analysis of three mutually orthogonal holes using displacements generated from (13), that is, synthetic data, are given in Tables 12, 13 and 14 using a BSM. Finite element results are in the 0-60-120 and 0-45-90 rows. Data in the FORMULA row are exact, that is, computed from the above formula (13).

Table 12. Stress Test Results using Synthetic Data for a Vertical Hole, LFM.

STRESS (MPa) METHOD	VERTICAL	EAST-WEST(	NORTH-SOUTH
0-60-120		84.17	96.86
0-45-90		81.72	91.40
FORMULA	60.69	83.45	94.83

A vertical hole does not give an indication of vertical stress in this analysis.

Table 13. Stress Test Results using Synthetic Data for an East-West Hole, LFM.

STRESS (MPa) METHOD	VERTICAL	EAST-WEST	NORTH-SOUTH
0-60-120	61.26		95.59
0-45-90	61.64		95.81
FORMULA	60.69	93.45	93.83

An east-west hole does not give an indication for the east-west normal stress.

Table 14 Stress Test Results using Synthetic Data for a North-South Hole, LFM.

STRESS (MPa) METHOD	VERTICAL	EAST-WEST	NORTH-SOUTH
0-60-120	61.26	83.74	
0-45-90	61.64	83.30	
FORMULA	60.69	83.45	94.83

A north-south hole does not give an indication for the north-south normal stress.

Inspection of the data in these three tables indicates agreement within a few percent of actual formula values. These results support the use of the FEP for monitoring and measuring stress change using a BSM in anisotropic rock

In fact, data from the Lucky Friday Mine involving 10 BSM's are available for illustrating application and for comparisons between Geokon results and finite element results. These gauges have two sets of sensors in 0-60-120 degree configuration separated but a few centimeters along the gauge. An expectation is the two sets of sensors will indicate very nearly the same hole diameter changes. However, plots show very different results; some sensors appear normal, others not so. Averaging of the two sets was therefore done for all 10 gauges to obtain consistent results and to avoid making arbitrary sensor selections for data reduction. Averages of BSME2 through BSM10 (vertical holes) in case of anisotropic rock and in case of isotropic rock are given in Table 15. The differences are not large, less than 17 percent in every category. Data in the table indicate a rough difference of 5 percent to16 percent between anisotropic and isotropic rock cases.

Table 15. Comparisons of BSM2 through BSM10 Vertical Hole Averages, LFM.

CASE STRESS (MPa)	ANISO.	ISO.	RELDIF(%)
ave SXX east/west	19.81	18.77	5.3
ave SYY north/south	14.26	12.76	10.6
ave TXY shear	-1.40	-1.19	15.3
ave S1 (major)	21.21	20.17	4.9
ave S3 (minor)	12.94	11.35	11.8
Angle θ (deg)*	-9.8	-7.8	20.6

*Measured positive counter-clockwise from the x-axis. Compression is positive.

A specific comparison of results for BSM6 installed 30.5 m (100 ft) down a vertical hole is presented in Table 16. Runstream files for these finite element analyses have the form given in Figure 19. The finite element data are computed using measured BSM6 diameter changes and finite element stiffnesses in case of isotropy and anisotropy. As the table shows, the differences between the isotropic and anisotropic finite element results for SXX and SYY are within about 11 percent. The shear stress difference is much higher because of the small shear stresses in both cases. Geokon stresses are based on the isotropic data reduction scheme described in a Geokon manual. The percentage differences between the Geokon and FEM results for SXX and SYY are within 10 percent, while the much smaller shear stresses again differ by a much greater percentage. Because of the shear stress difference, the angles θ are also noticeably different. The principal stresses S1 and S2 (P and Q in Geokon notation), are within ten percent as seen in the table under the % Relative Difference column. The gauge BSM6 has two sets of three sensors at 60 degree spacing. Ideally, the two sets give nearly the same readings, although the readings may also differ considerably in the harsh environment of a deep, underground hardrock mine. A reasonable approach is to use averages of the two sets and indeed averaging was done in the comparison data given in the table. Figure 21 shows BSM6 diameter change (radial change) for two sets of three sensors collected over a period of several years. Figure 22 shows averaged sensor data for comparison.

Table 16. Comparison of BSM6 results from finite element and Geokon computations. (FEM=finite element results, GEOKON=results from the Lucky Friday Mine).

METHOD/ QUANTITY	FEM iso MPa	FEM aniso- MPa/psi	GEOKON iso MPa/psi	% Rel Diff iso/aniso	% Rel Diff iso/GEOKON
SXX	16.47	17.64	16.04	6.66	2.57
SYY	14.28	15.98	13.14	10.63	8.01
TXY	0.61	3.12	1.03	80.35	-67.14
S1	16.62	20.04	16.37	17.04	1.55
S2	1412	13.58	12.81	-3.99	9.27
Θ (deg)	14.65	37.54	17.6	60.98	-20.15

There is an axial strain effect to be considered. Analysis proceeds initially under a plane strain assumption. However, a non-zero axial strain ε_{zz} may be present. Correction for this strain may be applied to diameter changes or to stress changes. When applied to changes in principal stress S1 and S2 or P and Q the correction is

$-Ev\varepsilon_{zz}/2$ where tension is positive, *E* is Young's modulus, and *v* is Poisson's ratio for isotropic rock. When the axial strain is compressive, the correction is an increase in stress. If the axial strain is not measured, then the correction may be ignored or an educated guess made. In case of anisotropic rock, the correction is more involved but still of the same size and may be estimated using average rock properties. In this regard, the comparison data in Table 8 are not corrected for axial strain, no axial strain correction was used.

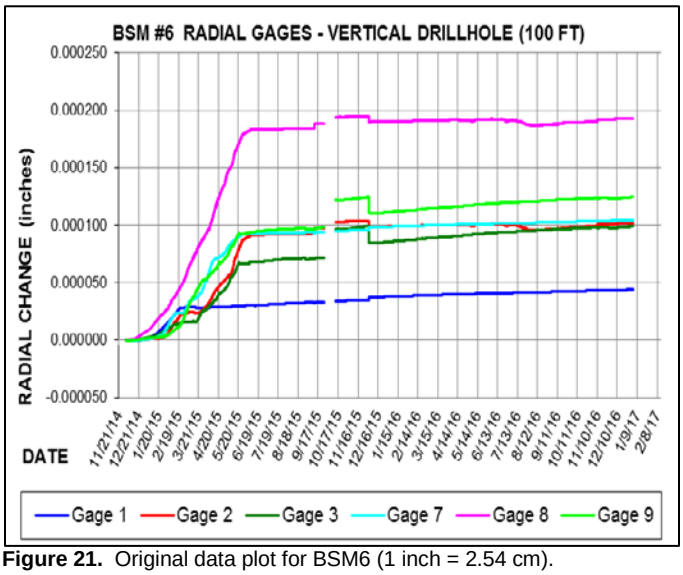

Figure 21. Original data plot for BSM6 (1 inch = 2.54 cm).

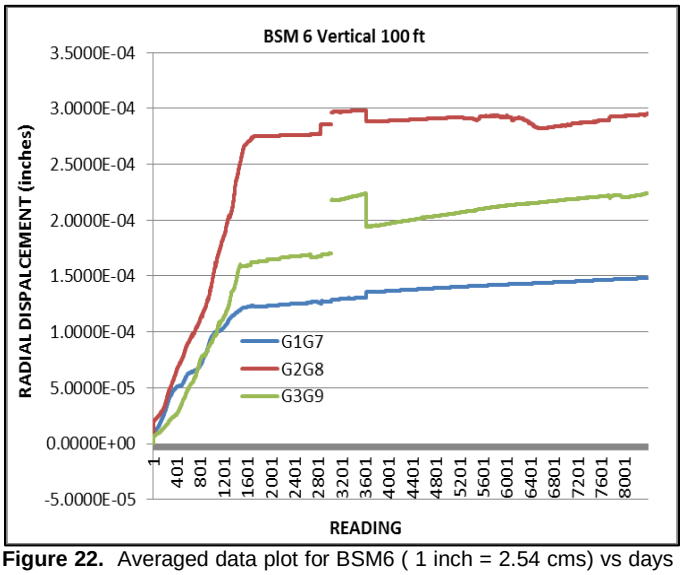

Figure 22. Averaged data plot for BSM6 (1 inch = 2.54 cms) vs days after installation.

APPLICATION TO BOREHOLE DEFORMATION GAUGES

Application of the FEP to stress monitoring and measurement in anisotropic rock using U.S. Bureau of Mines borehole deformation gauge data (BDG) demonstrates the new approach using data from HSM. A BDG does not affect hole wall displacements, so an open hole analysis is applicable. Analysis of a single hole illustrates the FEP first. A three hole analysis shows how the changes in borehole diameters leads to change in the three dimensional stress state in the vicinity of the boreholes and is well-developed technology[19].

Open Hole Analysis (BDG)

Consider the procedural formulation for stress monitoring and measurement that begins with expressions for displacements at the wall of a circular hole in terms of prehole stresses. Thus,

$$\begin{Bmatrix} u \\ v \end{Bmatrix} = [B] \begin{Bmatrix} \sigma^o_{xx} \\ \sigma^o_{xx} \\ \tau^o_{xy} \end{Bmatrix} \tag{16}$$

where *u* and *v* are x- and y-displacements, [*B*] is a 2x3 matrix of functions that are constants at a given point, the hole axis is parallel to the z-axis, and plane strain conditions in the vicinity of the gauge are assumed.

A forward finite element analysis gives the displacements on the left hand side of (11) associated with hole excavation in rock subject to the *in situ* stresses on the right hand side at all nodes at the hole wall.

A simple rotation about the hole axis (z-axis) gives the radial and tangential displacements at the hole wall. Thus,

$$\begin{Bmatrix} u_r \\ v_t \end{Bmatrix} = [B_r] \begin{Bmatrix} \sigma^o_{xx} \\ \sigma^o_{xx} \\ \tau^o_{xy} \end{Bmatrix} \tag{17}$$

In the analytical approach, the *b's* are unknown complex variable functions that are approximated by Fourier series . When evaluated at a point, the results of (17) must be the same as in the complex variable formulation.

With focus on radial displacement at the hole wall, one has

$$u_r = b_{11}\sigma^o_{xx} + b_{12}\sigma^o_{yy} + b_{13}\tau^o_{xy} \tag{18}$$

that suggests solution for the stresses using three values of hole wall displacements. For example, with the choice of angles 0, 45, and 90 degrees,

$$\begin{Bmatrix} u_r(0) \\ u_r(45) \\ u_r(90) \end{Bmatrix} = [B] \begin{Bmatrix} \sigma^o_{xx} \\ \sigma^o_{yy} \\ \tau^o_{xy} \end{Bmatrix}, \quad \begin{Bmatrix} \sigma^o_{xx} \\ \sigma^o_{yy} \\ \tau^o_{xy} \end{Bmatrix} = [B]^{-1} \begin{Bmatrix} u_r(0) \\ u_r(45) \\ u_r(90) \end{Bmatrix} \tag{14a,b}$$

and application of $\sigma^0_{xx} = -1000,\ \sigma^o_{yy} = -2000,\ \sigma^o_{zz} = 0$ $\tau^o_{yz} = 0,\ \tau^o_{zx} = 0,\ \tau^o_{xy} = -6000$ units of stress, hole wall displacements from a forward finite element analysis of the mesh shown in Figure 23 are: $u_r(0) = -0.0085,\ u_r(45) = -0.0294,\ u_r(90) = -0.0273$ units of displacement. Inversion of [*B*] with elements determined from the uniaxial stress to stiffness procedure gives

$$[B]^{-1} \begin{bmatrix} 370296.0227 & -272153.4049 & 213719.8223 \\ 223221.455 & -302056.2129 & 327605.5886 \\ -265911.889 & 537872.0283 & -276350.3024 \end{bmatrix} \tag{19}$$

and multiplication by the radial displacements returns the multi-axial stresses $\sigma^0_{xx} = -1000,\ \sigma^o_{yy} = -2000$ and: $\tau^o_{xy} = -6000$. The accuracy indicated in $[B]^{-1}$ to four decimal places is an artifact of computation, of course, and the results are constrained by the geometry of a quarter circle. However, the procedure in case of an otherwise arbitrary stress state appears sound and numerically accurate. The same procedure is certainly applicable to transversely

isotropic and to isotropic rock. Extension of this finite element procedure to one based on borehole diameter change is thus justified.

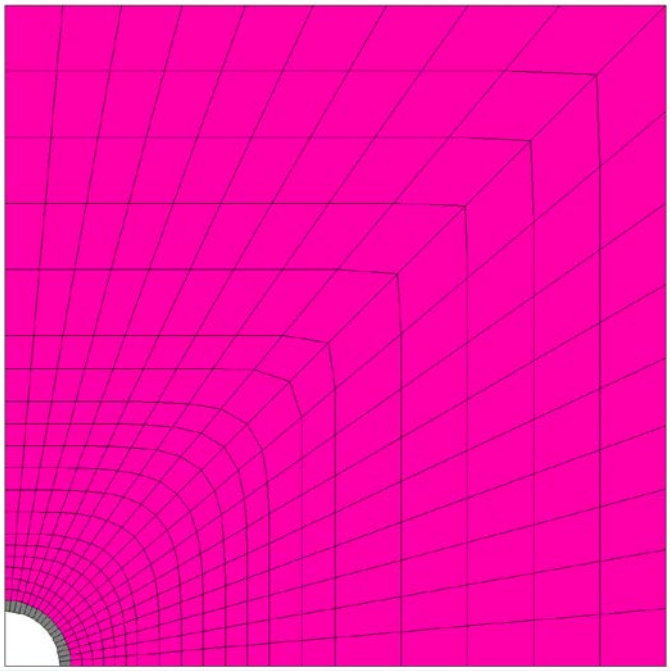

Figure 23. A circular hole in a three dimensional slab of anisotropic rock. Hole radius is 3 units to the colored elements. Grey elements are excavated air elements. The mesh has 19 nodes spaced at 5 degree intervals along the hole wall with. Hole radius is 7.62 cms; mesh width is 30 units, that is, ten times hole radius, so external boundaries are sufficiently remote to negate any influence on hole wall displacements. Symmetry about the horizontal and vertical axes prevails.

Rock properties used in obtaining these results were obtained in **anisotropic rock** (Poorman Formation) that forms the footwall of the gold ore-bearing Homestake Formation at the former Homestake gold mine in the Northern Black Hills of South Dakota. The Poorman, Homestake and Ellison (hanging wall) formations are Precambrian meta-sediments, mainly phyllites and schists (Slaughter 1968). The elastic and strength properties are given in Table 17. For demonstration purposes, the elastic moduli were reduced to one-tenth table properties; strength properties were increased by a factor of ten to ensure elastic behavior.

Table 17. Poorman Formation rock properties.

1 --(5) POORMAN N=2 a=down dip, b=strike, c=normal						**Key**
13.5E+06	7.2E+06	13.7E+06	0.23	0.15	0.22	*Ea Eb Ec vab vbc vca*
3.8E+06	3.9E+06	5.6E+06				*Gab Gbc Gca*
13630.0	10000.0	12270.0	2990.0	820.0	1910.0	*Ca Cb Cc Ta Tb Tc*
1500.0	2800.0	1280.0				*Ra Rb Rc*

The **Key** defines the properties: E=Young's moduli, v=Poisson's ratios, G=shear moduli, C=unconfined compressive strength, T=tensile strength, R=shear strength. The anisotropy is for a material with three planes of elastic symmetry (orthotropic model) and requires nine independent elastic properties (3 E's, 3 v's, 3 G's) and similarly for strengths (3 C's, 3 T's, 3 R's). In this analysis, the axes of anisotropy (*abc)* coincide with the finite element axes (*xyz*).

The sum of hole wall radial displacements spaced 180 degrees apart quantifies hole wall diameter change, that is,

$$\begin{aligned}\Delta D(\theta) &= u_r(\theta) + u_r(\theta+\pi) \\ &= (b_{11}\sigma^o_{xx} + b_{12}\sigma^o_{yy} + b_{13}\tau^o_{xy})_\theta + (b_{11}\sigma^o_{xx} + b_{12}\sigma^o_{yy} + b_{13}\tau^o_{xy})_{\theta+\pi} \\ \Delta D(\theta) &= b_{11}(\theta)\sigma^o_{xx} + b_{12}(\theta)\sigma^o_{yy} + b_{13}(\theta)\tau^o_{xy}\end{aligned} \tag{20}$$

Hence,

$$\begin{Bmatrix}\Delta D_1 \\ \Delta D_2 \\ \Delta D_3\end{Bmatrix} = [c]\begin{Bmatrix}\sigma^o_{xx} \\ \sigma^o_{yy} \\ \tau^o_{xy}\end{Bmatrix} \text{ and } \begin{Bmatrix}\sigma^o_{xx} \\ \sigma^o_{yy} \\ \tau^o_{xy}\end{Bmatrix} = [k]\begin{Bmatrix}\Delta D_1 \\ \Delta D_2 \\ \Delta D_3\end{Bmatrix} \tag{21a,b}$$

where[*c*] is a 3x3 compliance matrix and [*k*] is a 3x3 stiffness matrix which is the inverse of the compliance matrix.

Uniaxial application of the original -1000 units in a six run sequence followed by stiffness computations and then application of the multi-axial stress field used previously gives diameter changes using a full-circle mesh.

$$\begin{aligned}\Delta D(0) &= -0.0014 \\ \Delta D(45) &= -0.1082 \text{ displacement units} \\ \Delta D(90) &= -0.0226\end{aligned} \tag{22}$$

After application of (21a) the resulting stresses associated with the diameter changes (22) are

$$\begin{aligned}\sigma^o_{xx} &= -1000 \\ \sigma^o_{yy} &= -2000 \\ \tau^o_{xy} &= -6000\end{aligned} \tag{23}$$

An alternative set of diameter changes is

$$\begin{aligned}\Delta D(0) &= -0.01400 \\ \Delta D(60) &= -0.09981 \\ \Delta D(120) &= +0.6498\end{aligned} \tag{24}$$

Again, inversion after computation of the new node uniaxial stiffnesses returns close (within one percent) approximations to the original applied stresses in parentheses:

$$\begin{aligned}\sigma^o_{xx} &= -1002\ (-1000) \\ \sigma^o_{yy} &= -2004\ (-2000) \\ \tau^o_{xy} &= -6050\ (-6000)\end{aligned} \tag{25}$$

Why the 0-45-90 is more accurate than the 0-60-120 estimates of prehole stress is unknown but perhaps associated with the angular spacing of points. A loss of accuracy would be expected as the points become more closely spaced. To test this hypothesis, the procedure was applied to a set of points at 40, 45, and 50 degrees and also to a set at 115, 120, and 125 degrees. In both test cases, the errors were substantial, often over 100 percent, indicating ill-conditioning of the two systems. The underlying mathematical reason can be substantiated by calculating matrix condition numbers. A low condition number is indicative of a well-behaved system; a high condition number indicates potentially inaccurate matrix inversion. Indeed this was found to be the case. Condition numbers using four different norms were more than 100 hundred times in the 40-45-50 case than the same norms in the 0-45-90 case. Intuitively, widely spaced points would seem preferable, and indeed, this brief analysis shows such a preference to be the case.

HME Examples

Stress measurements made at the former Homestake gold mine in the northern Black Hills of South Dakota in conjunction with a shaft pillar mining project are available for use in testing the new finite element based technique (Johnson et al 1993). Rock mechanics studies at the mine over an extended period provide much information on rock properties data, *in situ* stresses, and the efficacy of forward

finite element modeling of stress field changes induced by mining (Pariseau et al 1995, 1996). The mine was developed to the 2,438 m (8,000 ft) level in Precambrian meta-sediments (phyllites, schists). The Homestake formation is ore-bearing; the Poorman and Ellison formations form the footwall and hanging wall, respectively. All show highly directional rock properties. Indeed an orthotropic anisotropy is present in all formations. The axes of anisotropy (*abc*) point down dip, on strike and normal to the foliation, respectively. Formation dip varies over a series of gently plunging folds from anticline to syncline. Assimilation of many stress measurements by various investigators working on different mine levels and different sections of the mine led to formulas that give reasonable estimates of the vertical and horizontal *in situ* stresses. Thus,

$$\begin{aligned} \sigma_V &= 0.283z \\ \sigma_H &= 143.31 + 0.120z \\ \sigma_h &= 8.34 + 0.124z \end{aligned} \tag{26}$$

where stress is in kPa and z is depth in meters, σ_V =vertical, σ_H = East-West, σ_h = North-South at the mine. With neglect of small shear stresses, these stresses (21) are principal stresses. Properties of the Homestake formation are given in Table 18.

Table 18. Homestake formation rock properties.

1 --(6) POORMAN N=2 a=down dip, b=strike, c=normal					
12.8E+06	9.3E+06	9.0E+06	0.14	0.18	0.19
4.8E+06	3.9E+06	4.3E+06	.00	.00	0.00
20150.0	11550.0	13270.0	1378.0	1140.0	1920.0
2050.0	2470.0	2100.0			
50.0	0.00	0.00			

Computation of borehole wall compliances and then stiffnesses using the open hole procedure described previous lead to estimates of the North-South and East-West stresses and to two estimates of the vertical stress.

The BDG used for measurement on the 3650 level following historical mining but prior to pillar mining responded to diameter changes at three diameters spaced at 60 degree intervals. Estimates of the North-South and East-West and Vertical stress were made using the acquired data[14]. In this case the changes in background stress are the prehole stresses.

Figure 24 shows the 3650 Level at the Homestake Mine where measurements were made and Figure 25 shows the data obtained using a BDG. In Figures 24 and 25, Hole 1 is A, Hole 2 is B and Hole 3 is C.

Comparisons of three estimates of stress are given in Table 19. The relative percentage differences between the formula based and finite element based (FEP) results are between three and twelve percent. However, the FORMULA and BDG estimates are based on isotropic rock; the FEP results assume anisotropic properties of the Homestake formation in which the measurement were made. In this comparison, the differences between isotropic and anisotropic data reductions are not significant; especially when data scatter in-hole and between-holes is considered. In this regard, the anisotropy of the Homestake formation seen in Table 18 is small with moduli differences of about 53 percent. A remark found in Obert and Duvall (1967) that if the ratio of moduli is less than two, then anisotropy can be neglected. However, this remark is based on differences in tensile stress concentration ranging from 24 to 32 percent and compressive stress differences ranging between 8 and 11 percent when the moduli ratio Young's moduli parallel and perpendicular to bedding is 1.31 and loading uniaxial. In any case, with the new capability to handle anisotropy, there is no reason not to account for it, although anisotropic rock properties data are required and pose an additional testing burden.

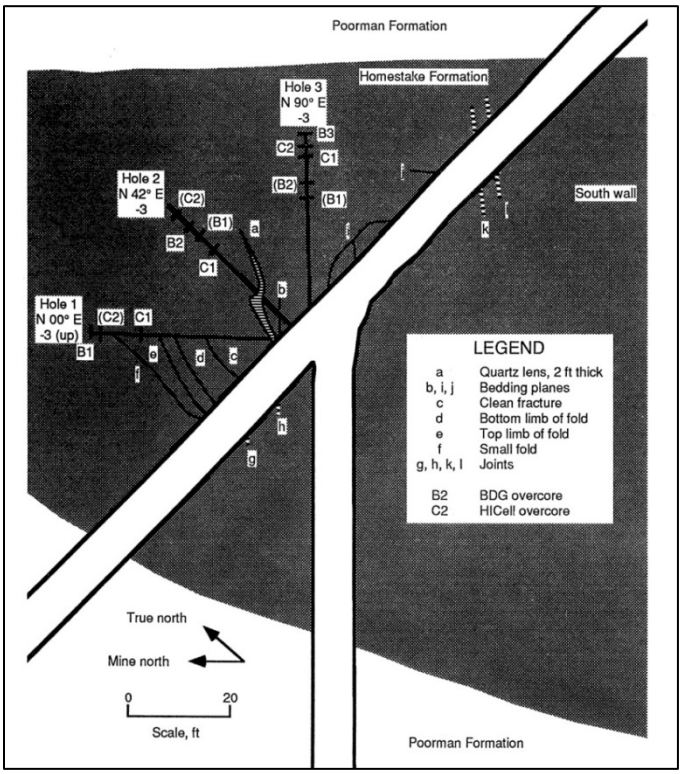

Figure 24. Borehole locations from USBM RI 9446.

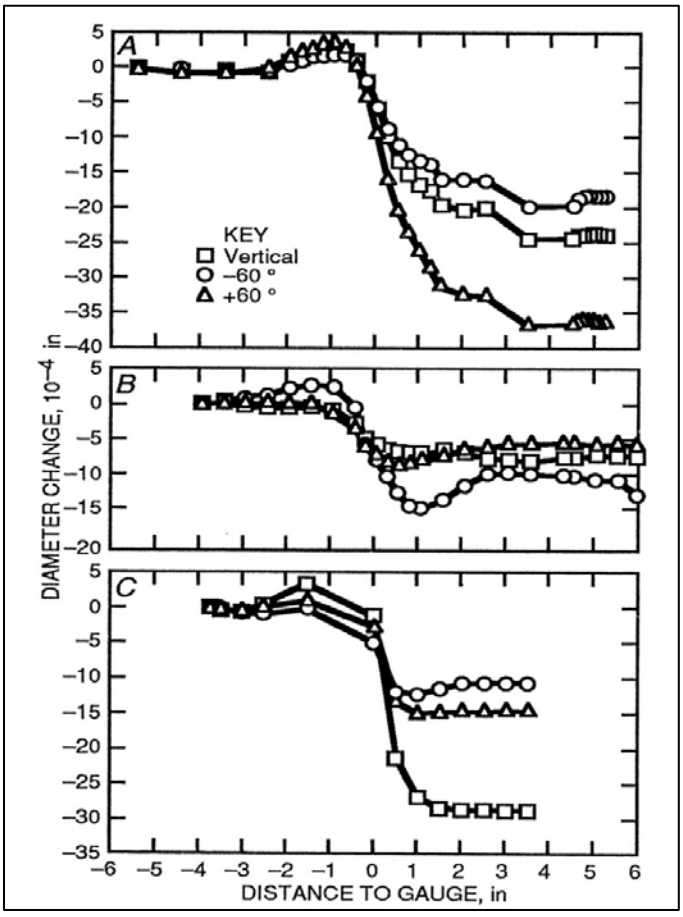

Figure 25 Borehole deformation data from USBM RI 9446 (1inch = 2.54 cms).

Table 19. Stress Estimation by Three Methods (MPa).

STRESS METHOD	VERTICAL	EAST-WEST	NORTH-SOUTH
FORMULA	31.69	27.68	14.68
BDG	35.66	32.76	19.52
FEP	27.94	31.02	15.08

Synthetic data also provide a worthwhile test of FEP, especially with three holes that are not co-planar. The test is to compute borehole wall stiffnesses for each hole and then to compute hole wall displacements using the Homestake stress formulas (21). These wall displacements are then used to compute associated stresses. The results should be just the original stresses given by (21). The stresses in (21) are principal stresses with neglect of any *in situ* shear stresses that measurements show to be an order of magnitude less than the normal stresses. At the 3650 Level, the stresses according to (21) are 14.68, 27.68 and 31.69 MPa in the east-west, north-south and vertical directions, respectively. These are just the FORMULA stresses in Table 19.

For this test, the foliation of the Homestake Formation is considered flat as it would be at the apex of an anticlinal fold or at the trough bottom of a synclinal fold. The three holes are aligned with the axes of anisotropy, east-west, north-south and vertical. Thus *abc* and *xyz* axes are aligned. However, all analyses are carried out in local, borehole coordinates, so rotations are still required. In all holes, the stresses are locally (σ_{xx}, σ_{yy}, τ_{xy}).

In the vertical hole, the global stresses are related by $\sigma_H = \sigma_{xx} = \sigma_{NS}$ and $\sigma_h = \sigma_{yy} = \sigma_{EW}$. In the east-west hole $\sigma_H = \sigma_{xx} = \sigma_{NS}$ and $\sigma_v = \sigma_{yy} = \sigma_{UP}$ and in the north-south hole $\sigma_h = \sigma_{xx} = \sigma_{EW}$ and $\sigma_v = \sigma_{yy} = \sigma_{UP}$. Shear stresses are absent because the three holes align with principal directions. This configuration poses a special challenge because of matrix inversion is usually a 3x3 task, but in this test, only a 2x2 inversion is possible. The FEP results for the three holes are given in Tables 19, 20, 21, and 22 for 0-60-120 degree and 0-45-90 degree angular positions for hole diameter change measurements using FEP.

Table 20. Stress Test Results using FEP Data for a Vertical Hole, Homestake Formation.

STRESS METHOD	VERTICAL MPa	EAST-WEST MPa	NORTH-SOUTH MPa
0 – 60 - 120		28.24	14.27
0 – 45 – 90		28.38	14.59
FORMULA	31.47	27.68	15.12

A vertical hole does not give an indication for vertical stress in this analysis.

Table 21. Stress Test Results using FEP Data for an East-West Hole, Homestake Formation.

STRESS METHOD	VERTICAL MPa	EAST-WEST MPa	NORTH-SOUTH MPa
0 – 60 - 120	30.26		14.12
0 – 45 – 90	31.52		14.44
FORMULA	31.47	27.68	15.12

An east-west hole does not give an indication for the east-west normal stress.

Table 22. Stress Test Results using FEP Data for a North-South hole, Homestake Formation.

STRESS METHOD	VERTICAL MPa	EAST-WEST MPa	NORTH-SOUTH MPa
0 – 60 - 120	29.61	27.81	
0 – 45 – 90	31.83	28.69	
FORMULA	31.47	27.68	15.12

No indication is given for the North-South stress in results from a north-south gauge hole.

Although not shown in the tables, there is an occasional small shear stress that appears in the results ranging from 0 to 1.15 MPa. The results from the synthetic data test show are within a few percent of the true (FORMULA) values and gives confidence in the overall procedure.

There is an axial strain effect to be considered and a decision to be made whether to include an axial strain adjustment. Analysis proceeds initially under a plane strain assumption. However, a non-zero axial strain ε_{zz} may be present. Correction for this strain may be applied to diameter changes or to stress changes. When applied to changes in principal stress S1 and S2 or P and Q the correction is $-E\nu\varepsilon_{zz} / 2$ where tension is positive, *E* is Young's modulus, and *v* is Poisson's ratio for isotropic rock. When the axial strain is compressive, the correction is an increase in stress. If the axial strain is not measured, then the correction may be ignored or an educated guess made. In case of anisotropic rock, the correction is more involved but still of the same size and may be estimated using average rock properties. In this regard, the comparison data are not corrected for axial strain in plane analyses; there is no need in a three dimensional analysis.

CONCLUSION

An outline of theory is presented and details are discussed for application of the well-known finite element method to stress measurement in *anisotropic* rock. Focus is on the popular Australian hollow inclusion cell (HI). The procedure is simple, based on fundamentals and implemented in three easy steps. The finite element based procedure is robust and applicable to rock whether isotropic, weakly anisotropic or strongly anisotropic. Any finite element program with anisotropic (orthotropic) capability, provision for initial stress and sequential excavation could be adapted to the data reduction process needed for anisotropic rock. The approach also overcomes the lack of a readily available analytical procedures based on a complex variable method. Data from four underground mines, three in hardrock and one in softrock, are used to demonstrate application of the method and the importance of anisotropic rock properties to *stress measurement*. Thus, a decades long gap in stress measurement technology is closed. Anisotropy does matter and to the extent that preexcavation stress is important to safe, stable excavation design, should be taken into account.

Measurements of hole wall diameter change using borehole stress meters and borehole deformation gauges allow for the determination of secondary principal stresses and their Cartesian components SXX, SYY and TXY where the *xy* plane is normal to the hole axis *z*. The data reduction procedure is well-known in case of *isotropic* rock and is based on elasticity theory and solution to a plane strain problem with possible correction for an axial strain effect. No such procedure is generally available in case of *anisotropic* rock, although the governing equations are the same with the exception of details in Hooke's law. Attempts at using stress functions of complex variables to solve the governing equations have not been fully substantiated nor replicated in the technical literature. Indeed, a serious disadvantage of such an approach is a potential division by zero in case of isotropic rock and potentially large errors in weakly anisotropic rock.

Finite element procedures (FEP) were developed that solve the governing equations of anisotropic elasticity, are easy to use, and produce accurate *in situ* stress changes from measurements in isotropic, transversely isotropic and anisotropic rock. Observations in two deep, underground mines in Precambrian meta-sediments show clear evidence of anisotropic effects on ground control requirements along drifts with the "grain" and crosscuts against the "grain" and indicate a need to consider anisotropy. Borehole stress meter data and borehole deformation gauge data from the two deep vein mines demonstrated the utility of the new finite element procedure in engineering practice. FEP can be extended to other types of gauges such as the popular Australian hollow inclusion gauge (HI-Cell) when used in anisotropic rock or *monitoring stress change*. The procedure is easily adapted to any finite element program which has anisotropic elastic analysis capability and avoids serious limitations associated with the complex variable approach

Additionally, the software described here is intended to be made available to the technical community at large on the website UT3PC.net which has user-friendly finite element programs for analysis of safety and stability of several important ground control problems in strata-bound mines and also for analysis of shafts and tunnels.

FUNDING

The study of stress measurement was done in cooperation with the Spokane Mining Research Division NIOSH under contract 75D30110PO1172 with the author. The study of monitoring stress change was done in cooperation with the Spokane Mining Research Division NIOSH under contract 2002016M90180 with the author.

REFERENCES

Aadnoy, B.S. (1987) Continuum Mechanics Analysis of the Stability of Inclined Boreholes in Anisotropic Rock Formations. Ph.D. thesis. University of Trondheim. pgs 204.

Aadnoy, B.S. (1987) Continuum Mechanics Analysis of the Stability of Inclined Boreholes in Anisotropic Rock Formations. Ph.D. thesis. University of Trondheim. pgs 204.

Amadei, B. (1983) *Rock Anisotropy and the Theory of Stress Measurements.* Springer-Verlag, Berlin, pgs 478.

Amadei, B. (1984) In Situ Stress Measurements in Anisotropic Rock. *Int. J. Rock Mech. Min. Sci. & Geomech. Abstr.* Vol. 21, No. 6, pp 327-338.

Amadei, B and O. Stephansson (1997) *Rock Stress and its Measurement.* Chapman &Hall, London, pgs 490.

Bathe, K-L. (1982) *Finite Element Procedures in Engineering Analysis*. Prentice-Hll, Englewood Cliffs, New Jersey.

Cook, R. D. (1974) *Concepts and Applications of Finite Element Analysis*. John Wiley & Sons, New York.

Corthesy, R., M.H. Leite, C. Vezina, A.C. Ouellet (2016) Application of the Inverse Problem to Stress measurement Interpretation in Anisotropic Rock. *Proc 7th International Symposium on In-Situ Rock Stress;* pp 309-319.

Desai, C. S. and J.F. Abel (1972) *Introduction to the Finite Element Method, A Numerical Method for Engineering Analysis*. Van Nostrand Reinhold Company, New York.

Duncan Fama, M. E. and M. J. Pender (1980) Analysis of the Hollow Inclusion Technique for Measuring *In Situ* Rock Stress. *Int. J. Rock Mech. Min. Sci. & Geomech. Abstr.* Vol 17, No. 3, pp 137-146.

Engles, H., D. Zakharov and W. Becker (2001) The Plane Problem of An elliptically Reinforced Circular Hole in an Anisotropic Plate or Laminate. *Archive of Applied Mechanics*. Vol. 71, No. 9, pp 601-612.

Figueiredo, B., L. Lamas and J. Muralha (2009) Numerical Modelling for Interpretation of Stress measurements by Overcoring. *Proceedings of the ISRM International Symposium on Rock mechanics – SINOROCK 2009*

Fung, Y. C. (1965) *Foundations of Solid Mechanics.* Prentice-Hall, Englewood Cliffs, New Jersey.

Fung, Y. C. (1965) *Foundations of Solid Mechanics*. Prentice-Hall, Englewood Cliffs, New Jersey.

Golder Associates (2010) Geotechnical Engineering Services In-Situ Stress Measurement Deep Underground Science and Engineering Laboratory (prepared for South Dakota School of Mines and Technology, Rapid City, South Dakota).

Hakala, M. and J. Sjoberg (2006) A methodology for Interpretation of Overcoring Stress Measurements in Anisotropic Rock. Working Report 2006-99, Posiva Oy, Olkiluoto, Finland.

Jaunzemis, W. (1967) *Continuum Mechanics* Macmillan Company, New York.

Johnson, J.C., W.G. Pariseau, D.F. Scott and F.M. Jenkins (1993) *In Situ Stress Measurements near the Ross Shaft Pillar, Homestake* Mine*, South Dakota.* U.S. Bureau of Mines Report of Investigations 9446.

Johnson, J. C., T. Brady, M. MacLauglin, R. Langston and H. Kirstern (2003) In situ Stress Measurements at the Stillwater Mine, Nye, Montana. *Proc 12th Pan-American Conference on Soil Mechanics and Geotechnical Engineering and the 39th U.S. Rock Mechanics Symposium, Massachusetts Institute of Technology*, Cambridge, Massachusetts, June, Vol. 1.

Johnston, E. D. (1968) The Chromite Deposits of the Stillwater Complex, Montana. *Ore Deposits in the United States 1933/1967* (ed:J. D. Ridge) Vol. II, AIME, New York.

Johnson, J.C, A. Arkoosh, M. Stepan, H. Abraham, D. Benton, C. Sunderman, M. Powers, S. Finley, B. Seymour and L. Martin. (2016) Rock Properties at the Lucky Friday Mine Biaxial Stress Measurement Site #1. Draft Report, OMSHR/SMRD Ground Control Branch.

Karpfinger, F., R. Prioul, O. Gaede, J. Jocker (2011) Revisitng Borehole Stresses in Anisotropic Elastic Media: Comparison of Analytical Versus Numerical solutions. *Proc. 45th U.S. Symposium on Rock Mechanics.* American Rock Mechanics Association, Paper 11-273.

Larson, M. K. (1987) An Experiment Using the Hicell for Stress Measurements in a Utah Coal Mine. M.S. thesis, University of Utah, Salt Lake City, Utah.

Larson, M. K (1992) STRESsOUT – A Data Reduction Program for Inferring Stress State of Rock Having Isotropic Material Properties: A User's Manual. USBM IC 9302.

Lekhnitskii, S.G. (1963) *Theory of Elasticity of an Anisotropic Elastic Body* (Translated from Russian by P. Fern). Holden-Day, San Francisco, pgs 404

Love, A. E. H. (1944) *A Treatise on the Mathematical theory of Elasticity* (4th edition) Dover Publications, New York.

Lu, M. (2006) Interpretation of In-situ Rock Stress measurement by Overcoring. *In-situ Rock Stress measurement, Interpretation and Application* (Proceedings of the International Symposium on In-situ Rock Stress: eds. M. Lu, C.C. Li, H. Kjorholt and H. Dahle). Taylor & Francis, London. pp 399-408.

Malvern, L. E. (1969) *Introduction to the Mechanics of a Continuous Medium*. Prentice-Hall, Englewood Cliffs, New Jersey.

Mining Plan Decision Document, Gordon Creek No. 2 Mine Beaver Creek Coal Company Carbon County, Utah. U.S. Department of the Interior, Office of Surface Mining Reclamation and Enforcement, August 1984.

Muskhelishvili, N.I. (1963) *Some Basic Problems of the Mathematical theory of Elasticity* (Fourth corrected and augmented edition, Moscow 1954). Translated by J.R. M. Radok, P. Noordhoff, Croningen, The Netherlands.

Obert, L. and W. I. Duvall (1967) *Rock Mechanics and the Design of Structures in Rock*. John Wiley & sons, Inc., New York.

Oden, J. T. (1972) *Finite Elements of Nonlinear Continua*. McGraw-Hill, New York.

Pariseau, W. G. and B. Voight (1970) "State of the Predictive Art in Subsidence Engineering," W. G. Pariseau and B. Voight, *J. of the Soil Mech. and Foundations Div.*, (Proc. ASCE, 96, SM2, 7210750, pp 721-750.

Pariseau, W. G. and K. Stout (1972) "Open Pit Mine Slope Stability: The Berkeley Pit," W. G. Pariseau and K. Stout, *Stability of Rock Slopes* (R. J. Cording, ed), Am. Soc. Civil Engrs, NY, pp 367-395.

Pariseau, W. G. M. K. Fowler, J. C. Johnson, M. Poad and E. L. Corp (1984) "Geomechanics of the Carr Fork Mine Test Stope," *Geomechanics Applications in Underground Hardrock Mining,* SME/AIME, NY, 1984.

Pariseau, W.G. (1985) Research Study on Pillar Design for Vertical Crater Retreat (VCR) Mining. U. S. Bureau of Mines Final Report. Contract JO215043.

Pariseau, W. G. (1987) An Alternative Solution for the In Situ Stress State Inferred from Borehole Stress Relief Data. *Proc. Sixth International Congress on Rock Mechanics*, Vol. 2, Balkema, Rotterdam, pgs 1201-1205.

Pariseau, W. G., J. C. Johnson and S. Orr (1990) "Three-dimensional Analysis of a Shaft Pillar at the Homestake Mine," *Proc. 31st U.S. Symp. on Rock Mechanics*, Balkema, 1990, pp 529-536.

Pariseau, W. G. (1994) "Design Considerations for Stopes in Wet Mines," W. G. Pariseau, *Proc. 12th Annual GMTC Workshop on Mines Systems Design and Ground Contro*l, pp. 37-48.

Pariseau, W.G. J.C. Johnson, M.M. McDonald and M.E. Poad (1995, 1996) *Rock Mechanics Study of Shaft Stability and Pillar Mining, Homestake Mine, lead, SD* (In Three Parts): 1. Premining Geomechanical Modeling Using UTAH2, 2Mine Measurements and Confirmation of Premining Results. 3. Geomechanical Monitoring and Modeling Using UTAH3.

Pariseau, W. G., S. C. Schmelter and A. K. Sheik (1997)"Mine Slope Stability by Coupled Finite Element Analysis," *Int'l J. Rock Mech. Mng Sci.*, Vol. 34, No. 3/4, paper no. 520.

Pariseau, W. G. and T. C. Trancynger (2012) Rock Mechanics of the Davis Detector Cavern. Society of Mining, Metallurgy and Exploration Preprint 12-022. 2012 SME Annual Meeting and Exhibit, Seattle, Washington, February 19-22 CD.

Pariseau, W. G. (2017)"Design Guidelines for Foundations on Jointed Rock", *Proc. 51st U.S. Symp. On Rock Mechanics.*, June 25-27, San Francisco.

Rahn, W. (1984) Stress Concentration Factors for the Interpretation of "Doorstopper" Stress Measurements in Anisotropic Rocks. *Int. J. Rock Mech. Min. Sci. & Geomech. Abstr.* Vol. 21, No. 6, pp 313-326.

Savin, G. N. (1961) *Stress Concentration Around Holes*. Oxford, Pergamon, pp 234-239.

Segerlind, L. J. (1976) *Applied Finite Element Analysis*. John Wiley & Sons, New York.

Slaughter, A.L. (1968) The Homestake Mine. *Ore Deposits in the United States 1933/1967* (J.D. Ridge, ed.) Vol. II, The American Institute of Mining, Metallurgical, and Petroleum Engineers, Inc. New York, pp1436-1459

Sokolnikoff, I. S. (1956) *Mathematical Theory of Elasticity*. McGraw-Hill, N.Y. pgs 476.

Ting, T.C.T. (1996) *Anisotropic Elasticity Theory and Applications*. Oxford University Press, N.Y., pgs 570.

Yameogo, S.T., R. Corthesy and M.H. Leite (2013a) Influence of Local Heterogeneity on Doorstoppper Stress Measurements. *International Journal of Rock Mechanics & Mining Sciences.* Vol. 60, pp 238-300.

Yameogo, S.T., R. Corthesy and M.H. Leite (2013b) Influence of Rock Failure and Damage on In Situ Stress Measurements in Brittle Rock. *International Journal of Rock Mechanics & Mining Sciences.* Vol. 61, pp 118-129.

Whyatt, J. K. and M. J. Beus (1995a) In Situ Stress at the Lucky Friday Mine (in Four Parts: 1 Reanalysis of Overcore Measurements from 4250 Level. USBM R1 9532.

Whyatt, J. K., F. M. Jenkins and M. K. Larson (1995b) In Situ Stress at the Lucky Friday Mine (in Four Parts): 2 Analysis of Overcore Measurement from 5300 Level. USBM R1 9560.

Whyatt, J. K., M. J. Beus and M. K. Larson (1995c) In Situ Stress at the Lucky Friday Mine (in Four Parts): 3. Reanalysis of Overcore Measurements from the Star Mine. USBM R1 9567.

Whyatt, J. K., T. J. Williams and W. Blake (1995d) In Situ Stress at the Lucky Friday Mine (in Four Parts): 4. Characterization of Mine In Situ Stress Field. USBM R1 9582.

Worontniki, G. and R. J. Walton (1976) "Hollow Inclusion gauges for the Determination of Rock Stress *In situ*" *Proc. ISRM Symp. on Investigaton of Stress in Rock and Advances in Shear Mesurement.* Sydney Supplement, pp 1-8.

Worotnicki, G, (1993) *Comprehensive Rock Engineering* (ed: J. A. Hudson), Volume 3, Chapter 13, Pergamon Press, Oxford, U.K. pp 329-394

Zienkiewicz and Y. K. Cheung (1967) *The Finite element Method in Structural and Continuum Mechanics.* McGraw-Hill, London.

Zienkiewicz, O. C. (1977) *The Finite Element Method* (3rd edition). McGraw-Hill, London.

APPENDIX A FINITE ELEMENT PROGRAM RELIABILITY

Reliability of the finite element approach to HI data reduction was demonstrated in detail by comparisons of numerical results with theory in two cases, a plane strain case and an anti-plane case; both are isotropic cases. Theoretical solution details are found in Jaeger and Cooke (1969), although the anti-plane solution required some adaptation. There are six unit loadings to consider.

Regression analyses substantiate the quite reasonable agreement between finite element results and theory. Figure A1 shows regression analysis results for the tangential (STT) and radial (SRR) normal stresses and the shear stress (TRT) also seen in cross-section in elements at the hole wall. These results also indicate a satisfactory finite element mesh that has suitable refinement at the hole wall.

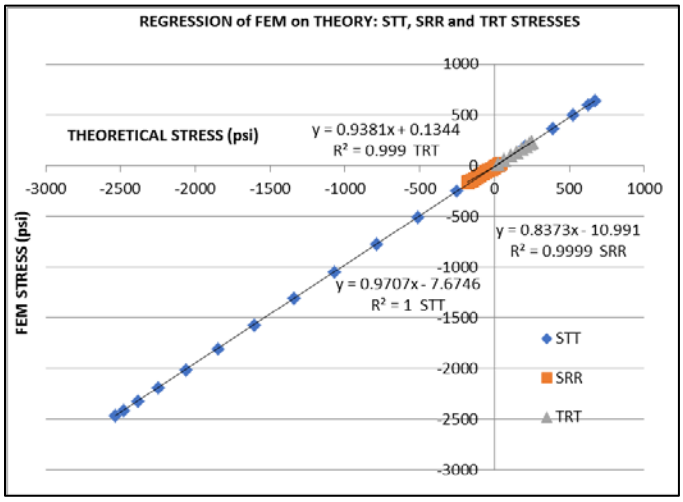

Figure A1. Regression analysis of finite element on theoretical results in case of isotropy.

Six unit load simulations of continuing the overcore past the HI lead to computation of the gauge compliance matrix [*S*] necessary for data reduction using $\{\sigma_h\} = [S]\{\varepsilon_g\}$ where the gauge strains $\{\varepsilon_g\}$ are computed from element strains $\{\varepsilon_e\}$. The computation is done in *xyz* (HI hole) coordinates where *z* is the hole axis. Cylindrical coordinates *rθz* are used to locate three-gauge rosettes. If gauge strains obtained under unit loadings are substituted in the data reduction equation, then the unit loadings should be recovered. This is indeed the case.

A concept using unit loads in a finite element scheme and somewhat similar to the one described here is presented by Corthesy *et al* (2016) in a context of the famous doorstopper stress gauge. However, the study was done in the laboratory; no application to an actual underground excavation is mentioned.

Several example calculations of isotropic and anisotropic rock illustrate the finite element approach to stress measurement using an Australian HI Cell with nine strain gauges in. These calculations raised some doubt about the standard HI Cell data reduction scheme described by Duncan Fama and Pender (DF-P, 1980). There was some disagreement with results from the standard, analytical data reduction method in the case of isotropy. In this regard, there appears to be no independent verification of the DF-P (1980) formulation in the technical literature. The computer program STRESsOUT comes close (Larson 1992). However, differences in results amongst the three methods (FEM, DF-P and STRESsOUT) remain unexplained.

APPENDIX B EFFECT OF CEMENT

The effect of cement properties on gauge performance can be assessed by doing analyses with all factors the same except cement properties. Three test cases using cement properties equal to: (i) HI properties, (ii) an order of magnitude smaller than HI properties, and (iii) an order of magnitude larger than HI properties, corresponding to standard, flexible and stiff cement, so to speak. Rock and HI properties are given in Figure 3 in the first example calculation using the finite element procedure.

Figure B1 shows in cross section a portion of the finite element mesh used in a brief study of cement effects on results of stress measurements using an HI. The HI is similar but not identical to the Australian triaxial stress measurement cell described in detail by Worotnicki (1993). Worotnicki gives a detailed account of cell manufacture and use and further describes effects of cement properties and thickness on stress measurements through effects of the *K* factors used in reducing data obtained in isotropic rock. He allowed cement to have moduli ranging for 1/4th to 4 times HI moduli. The effects according to boundary element and finite element modeling vary with HI thickness and cement thickness as well as with elastic moduli. These effects were quantified in terms of the parameters K_1 and K_2; which relate to in-plane principal stress sums and difference. Effects on K_3 and K_4 which relate to the axial stress and shear stresses were not evaluated. He concludes that cement with elastic moduli less than HI moduli ("soft" cement) leads to stresses less than if the cement had the same moduli as the HI. Stiff cement appeared to have little effect according to Worotnicki.

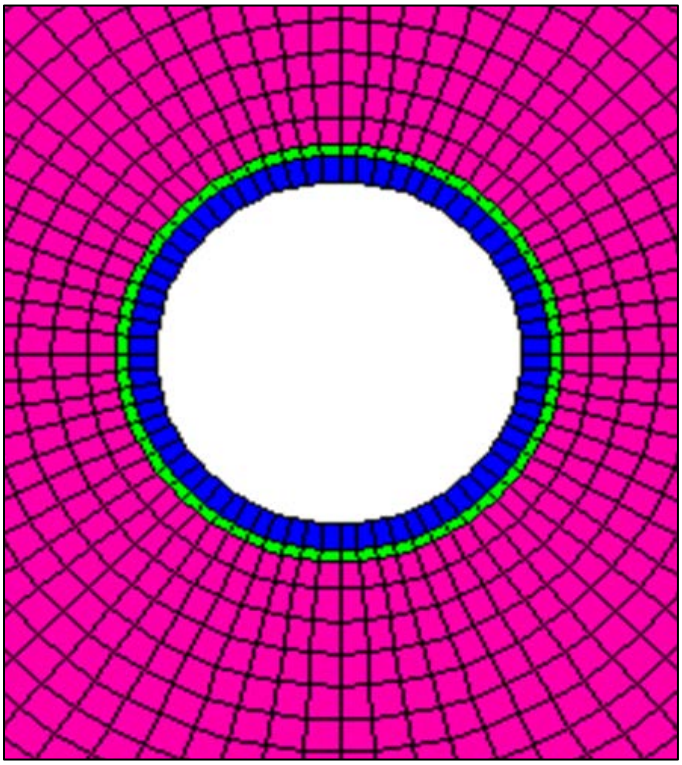

Figure B1. Cross section close-up through an HI cemented in a drill hole. Hole diameter is 39 mm. Inside diameter of the HI is 32 mm. HI thickness is 2.5 mm (blue). Cement thickness is 1 mm (green). Rock is red.

Six finite element models of gauge installation and subsequent overcoring were used to assess cement moduli effects on data reduction to stress in situ. Three analysis used equal stresses (Sxx=Syy=…Txy=1) and three used unequal stresses in descending value (Sxx=6, Syy=5,...,Txy=1). Both sets used the three values of elastic moduli of cement (flexible, same, stiff). The results are shown in Figure B2.

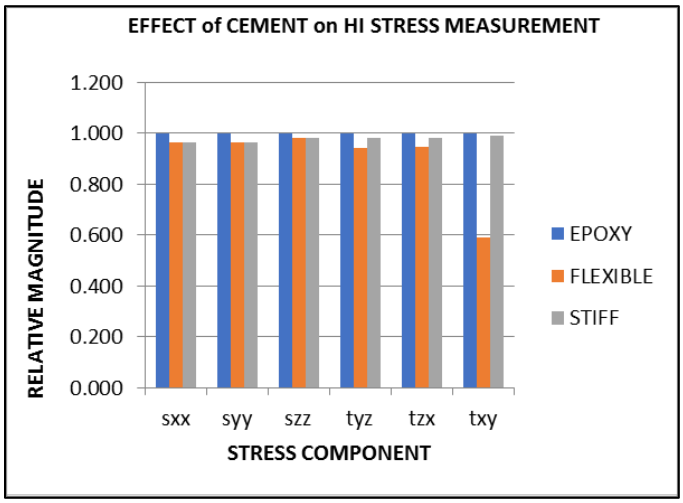

(A)

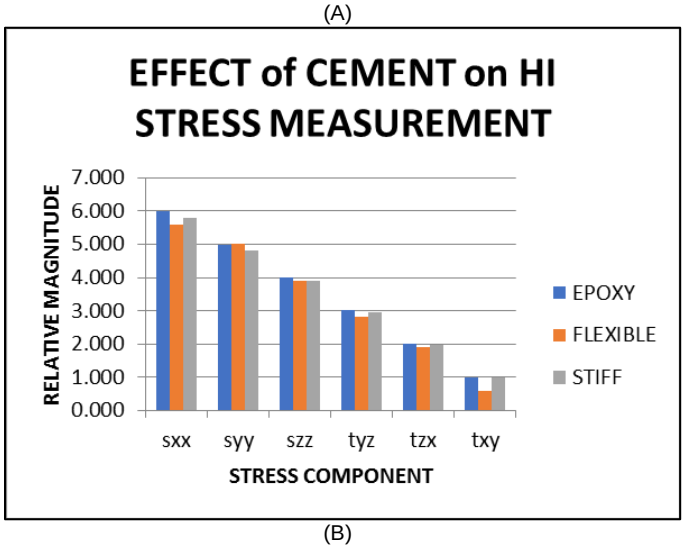

(B)

Figure B2. Effect of cement properties (elastic moduli) on stress measurements using an HI with elastic moduli of EPOXY (blue). FLEXIBLE (red)=cement moduli of 1/10th epoxy moduli, STIFF (green)=cement moduli 10X epoxy moduli. (A) applied stresses are equal (sxx=syy=…=txy=1) (B) applied stresses are in a descending order (sxx=6, syy=5,…,txy=1)

These results indicate stiff cement properties have little effect on measurement outcomes, while flexible cement may have a large effect. As a practical matter, cement with elastic moduli less than that of epoxy seems unlikely; cement moduli larger than epoxy moduli seems much more likely to be the case. Thus, the tacit assumption in HI data is reduction that the cement has the same properties as the epoxy and therefore no provision for introduction of cement properties is necessary. However, the finite element procedure described here allows for cement and epoxy to have different properties in any case by simple specification in the input material properties file.